

Polynomial curvelets on higher-dimensional spheres

Frederic Schoppert *

Institute of Mathematics, University of Lübeck, Ratzeburger Allee 160, 23562,
Lübeck, Germany

Abstract

In this article, we introduce and investigate polynomial curvelets on spheres, which form a class of Parseval frames for $L^2(\mathbb{S}^{d-1})$, $d \geq 3$. The proposed construction offers a directionally sensitive multiscale decomposition and provides a sparse representation of spherical data. As a main result, we derive a sharp pointwise localization bound which shows that the frame elements decay rapidly away from their center of mass, making them a powerful tool for position-based analyses. In contrast to previous constructions, polynomial curvelets are not limited in their directional resolution. Consequently, the frames established in this article are particularly powerful when it comes to the analysis of localized anisotropic features, such as edges. To illustrate this point, we show that, given a suitable test signal that exhibits (higher-order) discontinuities at the boundary ∂A of a spherical cap $A \subset \mathbb{S}^{d-1}$, the corresponding curvelet coefficients peak precisely when the analysis function matches some segment of the boundary ∂A , both in terms of position and orientation. Otherwise, the coefficients decay rapidly.

Keywords: Curvelets; Sphere; Directionality; Parseval frame; Localization; Edge detection.

1 Introduction

In a recent article [14], we introduced a general class of polynomial frames for $L^2(\mathbb{S}^{d-1})$, $d \geq 3$. This class includes the well-established zonal (isotropic) systems, sometimes called spherical needlets (see e.g. [1, 10, 11, 13, 18, 19, 20, 22, 24, 25, 26]), but also paves the way for a variety of new anisotropic (non-zonal) designs. Based on this newly established framework, we introduce a family of highly directional and localized Parseval frames for $L^2(\mathbb{S}^{d-1})$, $d \geq 3$. These frames extend the two-dimensional construction of second-generation curvelets presented in [9], and they provide a tool for position-frequency analyses of spherical data, offering additional directional resolution at each scale and position. Unlike previous constructions, we show that the polynomial curvelets defined in this article are not limited in their directional sensitivity and they can be used to precisely identify localized features, such as edges, not only in terms of their position but also in terms of their orientation.

On the 2-sphere, localized directional polynomial frames were previously established in the form of so-called directional wavelets [16, 17, 35] and second-generation curvelets [9]. Due to their excellent spatial localization and directional sensitivity, both systems have found a variety of applications in the analysis of spherical random fields (e.g. [2, 15, 16, 27, 28, 36]), often related to problems in cosmology. Further areas of relevance include

*f.schoppert@uni-luebeck.de

sparse reconstruction (e.g. [33]), image segmentation (e.g. [8]), as well as the detection of (higher-order) discontinuities in signals [29, 31].

The general framework established in [14] includes the aforementioned directional wavelets and second-generation curvelets as special cases and, moreover, allows us to extend these systems to higher-dimensional spheres. For directional wavelets, an extension to \mathbb{S}^{d-1} , $d \geq 3$, was studied in [30], resulting in a class of well-localized Parseval frames for $L^2(\mathbb{S}^{d-1})$, with adjustable (but limited) directional sensitivity. Here, the corresponding frames are generated by an initial sequence of polynomials $\Psi^j \in \Pi_{2^j}(\mathbb{S}^{d-1})$, $j \in \mathbb{N}_0$, that are highly concentrated at the North Pole e^d . Specifically, it was shown that

$$|\Psi^j(\eta)| \leq \frac{c_q 2^{j(d-1)}}{(1 + 2^j \text{dist}(\eta, e^d))^q}, \quad \eta \in \mathbb{S}^{d-1}, \quad (1)$$

for each $q \geq 1$ [30, Theorem 4.1]. For corresponding zonal frame functions, often called spherical needlets, this kind of localization bound is well-known (see [7, 11, 25, 26]). Moreover, in the special case $d = 3$, the estimate (1) was first proven in [31] for directional wavelets on \mathbb{S}^2 , and prior to that a slightly weaker version was shown in [16].

In this article, we extend the two-dimensional second-generation curvelets introduced in [9] to higher-dimensional spheres, by following the general construction in [14]. Specifically, for $d \geq 3$, we define an initial sequence $(\Psi_C^j)_{j=0}^\infty$ of polynomial curvelets satisfying $\Psi_C^0 \equiv 1$ and $\Psi_C^j \in \Pi_{2^j}(\mathbb{S}^{d-1})$ for each $j \in \mathbb{N}$. By using suitable rotation matrices $g_{j,r} \in SO(d)$ with corresponding weights $\mu_{j,r} > 0$, which arise from positive quadrature rules for spherical polynomials (see the discussion in Section 3), we obtain tight (Parseval) frames for $L^2(\mathbb{S}^{d-1})$ that are of the form

$$\mathcal{X}[(\Psi_C^j)_{j=0}^\infty] = \{\sqrt{\mu_{j,r}} \Psi_C^j(g_{j,r}^{-1} \cdot), r = 1, \dots, r_j, j \in \mathbb{N}_0\}.$$

Thus, each $f \in L^2(\mathbb{S}^{d-1})$ can be expanded into the polynomial curvelets $\Psi_C^j(g_{j,r}^{-1} \cdot)$ via

$$f = \sum_{j=0}^{\infty} \sum_{r=1}^{r_j} \mu_{j,r} \langle f, \Psi_C^j(g_{j,r}^{-1} \cdot) \rangle_{\mathbb{S}^{d-1}} \Psi_C^j(g_{j,r}^{-1} \cdot).$$

Indeed, we show that this frame expansion converges fast in $L^p(\mathbb{S}^{d-1})$, $1 \leq p < \infty$, and $C(\mathbb{S}^{d-1})$, provided that f belongs to the corresponding Banach space.

As a main result of the investigations presented in this article, we prove that polynomial curvelets satisfy the direction-dependent localization bound

$$|\Psi_C^j(x)| \leq \frac{c_q 2^{j(3d-2)/4} |x_d + ix_{d-1}|^{2^{j-1}}}{(1 + 2^j |\text{Arg}(x_d + ix_{d-1})|)^q}, \quad x = (x_1, \dots, x_d) \in \mathbb{S}^{d-1}, \quad (2)$$

for each $q \in \mathbb{N}$. Here, for $z \in \mathbb{C} \setminus \{0\}$, $\text{Arg}(z)$ denotes the unique element in $(-\pi, \pi]$ such that $z = |z| \exp(i \text{Arg}(z))$. The upper bound in (2) implies, in particular, that the functions Ψ_C^j are highly localized at the North Pole e^d . For two-dimensional curvelets [9], i.e., in the case $d = 3$, this estimate was previously established in [29, Proposition 2.4].

In contrast to other polynomial frames for $L^2(\mathbb{S}^{d-1})$, the polynomial curvelets constructed in this article are, just like in the two-dimensional setting [9, 29], not limited in their directional sensitivity. To reinforce this point, we derive an explicit formula for the auto-correlation functions

$$SO(d-1) \rightarrow \mathbb{C}, \quad h \mapsto \langle \Psi_C^j, \Psi_C^j(h^{-1} \cdot) \rangle_{\mathbb{S}^{d-1}}, \quad j \in \mathbb{N}_0,$$

which we observe to be highly concentrated at the identity matrix for large scales j . Here, we identify $SO(d-1)$ with the subgroup $\{h \in SO(d) : he^d = e^d\}$ of $SO(d)$. The price paid for the extra directional resolution is an increased computational cost. Specifically, the number of rotations needed at each scale j grows like $2^{j(2d-3)}$, whereas for previously considered polynomial frames it typically scales like $2^{j(d-1)}$.

To conclude this article, we demonstrate the effectiveness of polynomial curvelets when it comes to the detection of edges and higher-order singularities. Here, we consider a class of test signals f , which are smooth except for a (higher-order) discontinuity along the boundary ∂A of some spherical cap $A \subset \mathbb{S}^{d-1}$. In the simplest case, f is just the characteristic function of A , i.e., $f = \mathbf{1}_A$. We then prove that the frame coefficients $\langle f, \Psi_C^j(g^{-1}\cdot) \rangle_{\mathbb{S}^{d-1}}$, $g \in SO(d)$, peak when the rotated analysis function $\Psi_C^j(g^{-1}\cdot)$ matches some segment of the boundary ∂A in terms of position and orientation. If $\Psi_C^j(g^{-1}\cdot)$ is located away from ∂A , or if the orientation of $\Psi_C^j(g^{-1}\cdot)$ does not match the orientation of the closest edge segment, the inner products decay rapidly. The latter also underlines the (expected) sparsity of the curvelet representation. We note that in the two-dimensional context, i.e., for $d = 3$, the results presented have previously been established in [29].

The remainder of this article is structured as follows. In Section 2, we briefly review some fundamentals of harmonic analysis on \mathbb{S}^{d-1} , which will be essential for our investigations. The construction of Parseval frames consisting of polynomial curvelets is carried out in Section 3. In Section 4, we prove that the frame elements satisfy the direction-dependent localization bound in (2). In Section 5, we derive explicit expressions for the auto-correlation functions associated with polynomial curvelets, which point to a particularly strong directional sensitivity. Finally, in Section 6, we demonstrate the strength of polynomial curvelet frames when it comes to the problem of edge detection.

2 Preliminaries

Let $d \geq 3$. We consider the Euclidean space \mathbb{R}^d equipped with the usual inner product $\langle x, y \rangle = \sum_{i=1}^d x_i y_i$, as well as the corresponding induced norm $\|x\|_2 = \sqrt{\langle x, x \rangle}$. The canonical basis vectors of \mathbb{R}^d are given by $e^j = (\delta_{i,j})_{i=1}^d$, $j = 1, \dots, d$, where

$$\delta_{i,j} = \begin{cases} 1, & i = j, \\ 0, & i \neq j. \end{cases}$$

As usual, the unit sphere in \mathbb{R}^d will be denoted by $\mathbb{S}^{d-1} = \{x \in \mathbb{R}^d \mid \|x\|_2 = 1\}$ and we will refer to e^d as the North Pole of \mathbb{S}^{d-1} . The standard metric on \mathbb{S}^{d-1} is given by the geodesic distance

$$\text{dist}(\eta, \nu) = \arccos(\langle \eta, \nu \rangle), \quad \eta, \nu \in \mathbb{S}^{d-1}.$$

The set

$$C(z, \phi) = \left\{ x \in \mathbb{S}^{d-1} : \text{dist}(x, z) < \phi \right\}$$

constitutes a spherical cap with center $z \in \mathbb{S}^{d-1}$ and opening angle $\phi \in (0, \pi)$. It is sometimes beneficial to parameterize \mathbb{S}^{d-1} in terms of spherical coordinates $\theta_1 \in (-\pi, \pi]$,

$\theta_2, \dots, \theta_{d-1} \in [0, \pi]$, via

$$\eta(\theta_1, \theta_2, \dots, \theta_{d-1}) = \begin{pmatrix} \sin \theta_{d-1} \dots \sin \theta_2 \sin \theta_1 \\ \sin \theta_{d-1} \dots \sin \theta_2 \cos \theta_1 \\ \sin \theta_{d-1} \dots \sin \theta_3 \cos \theta_2 \\ \vdots \\ \sin \theta_{d-1} \cos \theta_{d-2} \\ \cos \theta_{d-1} \end{pmatrix}. \quad (3)$$

In the following, we will review some well-known concepts related to Fourier analysis on \mathbb{S}^{d-1} . For more information on this topic, we refer to [3, 11, 23, 32]. Let ω_{d-1} denote the usual rotation-invariant measure on \mathbb{S}^{d-1} which is normalized such that

$$\int_{\mathbb{S}^{d-1}} d\omega_{d-1} = 1.$$

In terms of spherical coordinates (3),

$$d\omega_{d-1} = \frac{\Gamma(\frac{d}{2})}{2\pi^{d/2}} \sin^{d-2} \theta_{d-1} \dots \sin \theta_2 d\theta_1 \dots d\theta_{d-1}.$$

With respect to this measure, the spaces $L^p(\mathbb{S}^{d-1})$, $0 < p < \infty$, are defined by

$$L^p(\mathbb{S}^{d-1}) = \{f: \mathbb{S}^{d-1} \rightarrow \mathbb{C} \mid f \text{ is measurable and } \|f\|_{L^p(\mathbb{S}^{d-1})} < \infty\},$$

where

$$\|f\|_{L^p(\mathbb{S}^{d-1})} = \left(\int_{\mathbb{S}^{d-1}} |f|^p d\omega_{d-1} \right)^{1/p}.$$

For notational convenience, we will use the symbol $L^\infty(\mathbb{S}^{d-1})$ to refer to the space of continuous functions $f: \mathbb{S}^{d-1} \rightarrow \mathbb{C}$, equipped with the supremum norm

$$\|f\|_{L^\infty(\mathbb{S}^{d-1})} = \sup_{\eta \in \mathbb{S}^{d-1}} |f(\eta)|.$$

Most investigations conducted in this article rely on Fourier methods which are available in the Hilbert space $L^2(\mathbb{S}^{d-1})$, where the inner product is given by

$$\langle f_1, f_2 \rangle_{\mathbb{S}^{d-1}} = \int_{\mathbb{S}^{d-1}} f_1 \overline{f_2} d\omega_{d-1}.$$

In particular, we will use a specific orthonormal basis of spherical harmonics (see [32, p. 466]), which has a convenient representation in terms of Gegenbauer polynomials

$$C_m^\lambda(t) = \frac{(-1)^m \Gamma(\lambda + 1/2) \Gamma(m + 2\lambda)}{2^m \Gamma(m + \lambda + 1/2) m!} (1 - t^2)^{1/2 - \lambda} \frac{d^m}{dt^m} (1 - t^2)^{m + \lambda - 1/2}, \quad \lambda > -1/2.$$

W.r.t. spherical coordinates (3), let

$$Y_k^{d,n}(\theta_1, \dots, \theta_{d-1}) = A_k^n \prod_{j=0}^{d-3} C_{k_j - |k_{j+1}|}^{\frac{d-j-2}{2} + |k_{j+1}|}(\cos \theta_{d-j-1}) \sin^{|k_{j+1}|}(\theta_{d-j-1}) e^{ik_{d-2}\theta_1}, \quad (4)$$

where $k_0 = n \in \mathbb{N}_0$ and $k = (k_1, \dots, k_{d-2}) \in \mathcal{I}_n^d$ with

$$\mathcal{I}_n^d = \{(k_1, \dots, k_{d-2}) \in \mathbb{N}_0^{d-3} \times \mathbb{Z} : n \geq k_1 \geq \dots \geq k_{d-3} \geq |k_{d-2}|\}.$$

The normalization constants $A_k^n > 0$ in (4) are defined by

$$(A_k^n)^2 = \frac{2^{(d-4)(d-2)}}{\Gamma(\frac{d}{2})} \prod_{j=0}^{d-3} \frac{2^{2|k_{j+1}|-j} (k_j - |k_{j+1}|)! (2k_j + d - j - 2) \Gamma^2(\frac{d-j-2}{2} + |k_{j+1}|)}{\sqrt{\pi} \Gamma(k_j + |k_{j+1}| + d - j - 2)}. \quad (5)$$

For $n \in \mathbb{N}_0$ and $k \in \mathcal{I}_n^d$, the function $Y_k^{d,n} \in L^2(\mathbb{S}^{d-1})$ defined above is a spherical harmonic of degree n . Moreover, the family $\{Y_k^{d,n}, k \in \mathcal{I}_n^d, n \in \mathbb{N}_0\}$ constitutes an orthonormal basis for $L^2(\mathbb{S}^{d-1})$. The spherical harmonic subspaces $\mathcal{H}_n^d = \text{span}\{Y_k^{d,n}, k \in \mathcal{I}_n^d\}$ are finite-dimensional with

$$\dim \mathcal{H}_n^d = \frac{(2n + d - 2)(n + d - 3)!}{(d - 2)!n!}. \quad (6)$$

By

$$\Pi_N(\mathbb{S}^{d-1}) = \bigoplus_{n=0}^N \mathcal{H}_n^d$$

we denote the set of spherical polynomials of degree $N \in \mathbb{N}_0$. With the above notation, every signal $f \in L^2(\mathbb{S}^{d-1})$ can be represented in terms of its Fourier series

$$f = \sum_{n=0}^{\infty} \sum_{k \in \mathcal{I}_n^d} f(n, k) Y_k^{d,n},$$

with the corresponding Fourier coefficients $f(n, k) = \langle f, Y_k^{d,n} \rangle_{\mathbb{S}^{d-1}}$.

Spherical harmonics satisfy the well-known addition theorem

$$\sum_{k \in \mathcal{I}_n^d} \overline{Y_k^{d,n}(\nu)} Y_k^{d,n}(\eta) = \frac{2n + d - 2}{d - 2} C_n^{\frac{d-2}{2}}(\langle \nu, \eta \rangle), \quad \nu, \eta \in \mathbb{S}^{d-1}, \quad (7)$$

which reveals a connection between harmonic analysis on the sphere \mathbb{S}^{d-1} and on the interval $[-1, 1]$. Indeed, for each fixed λ , the family $\{C_n^\lambda, n \in \mathbb{N}_0\}$ forms a complete orthogonal system for the Hilbert space $L^2([-1, 1], w_\lambda)$ w.r.t. the weighted inner product

$$\langle f_1, f_2 \rangle_{[-1,1], w_\lambda} = \int_{-1}^1 f_1(t) \overline{f_2(t)} w_\lambda(t) dt, \quad f_1, f_2 \in L^2([-1, 1], w_\lambda),$$

where $w_\lambda(t) = (1 - t^2)^{\lambda-1/2}$. Here, the Gegenbauer polynomials are normalized such that

$$\int_{-1}^1 |C_n^\lambda(t)|^2 w_\lambda(t) dt = \frac{\pi \Gamma(n + 2\lambda)}{2^{2\lambda-1} n! (n + \lambda) \Gamma^2(\lambda)}.$$

Thus, each $f \in L^2([-1, 1], w_\lambda)$ has an expansion of the form

$$f = \sum_{n=0}^{\infty} b_n^\lambda(f) C_n^\lambda, \quad (8)$$

where

$$b_n^\lambda(f) = \frac{2^{2\lambda-1}n!(n+\lambda)\Gamma^2(\lambda)}{\pi\Gamma(n+2\lambda)} \int_{-1}^1 f(t)C_n^\lambda(t)w_\lambda(t) dt. \quad (9)$$

Let $SO(d) = \{g \in \mathbb{R}^{d \times d} : g^\top = g^{-1}, \det g = 1\}$ be the special orthogonal group. For $g \in SO(d)$, we consider the rotation operator $T^d(g) : L^2(\mathbb{S}^{d-1}) \rightarrow L^2(\mathbb{S}^{d-1})$ given by

$$T^d(g)f = f(g^{-1}\cdot).$$

In fact, $g \mapsto T^d(g)$ defines a unitary group representation of $SO(d)$ on $L^2(\mathbb{S}^{d-1})$, which is irreducible on each spherical harmonic subspace \mathcal{H}_n^d . However, apart from some calculations in [Section 5](#), we will not refer to this property explicitly, although it plays an essential role in the background of this article. Indeed, the tools provided by the theory of harmonic analysis associated with the representation T^d constitute the foundation for several central results in [\[14\]](#), on which we will base our constructions. The material required for our investigations in [Section 5](#) is summarized in the [Appendix](#) of this article. For further details on the topic of harmonic analysis on $SO(d)$ associated with the rotation operators $T^d(g)$, $g \in SO(d)$, we refer to [\[32\]](#), as well as to our recent discussions in [\[14, 30\]](#).

In the following, for $m \in \{2, 3, \dots, d-1\}$, we will not distinguish between $SO(m)$ and the subgroup $\{h \in SO(d) : he^j = e^j \text{ for } j = m+1, \dots, d\} \subset SO(d)$. In particular, $SO(d-1)$ is identified with the subgroup of all elements in $SO(d)$ that keep the North Pole e^d fixed. For $\nu \in \mathbb{S}^{d-1}$, the symbol g_ν will always denote an arbitrary rotation matrix in $SO(d)$ such that $g_\nu e^d = \nu$. Likewise, if $\nu' \in \mathbb{S}^{d-2}$, we write $h_{\nu'}$ to refer to an arbitrary rotation matrix in $SO(d-1)$ satisfying $h_{\nu'} e^{d-1} = (\nu', 0) \in \mathbb{S}^{d-1}$.

Throughout this article, all constants c, c_0, c_1, \dots depend only on the dimension d and on the indicated parameters. Furthermore, their exact values might change with each appearance. For two non-negative sequences $(a_j)_{j=0}^\infty$ and $(b_j)_{j=0}^\infty$, we write $a_j \sim b_j$ to indicate that there exist constants $0 < c_1 \leq c_2$ such that

$$c_1 a_j \leq b_j \leq c_2 a_j, \quad \text{for each } j \in \mathbb{N}_0.$$

3 Construction of polynomial curvelets

The construction of polynomial frames presented in this chapter is motivated by the article [\[9\]](#), in which the authors defined highly directional analysis functions, so-called second-generation curvelets, on the 2-sphere. Specifically, utilizing the general framework recently developed in [\[14\]](#), we extend the systems considered in [\[9\]](#) to higher-dimensional spheres. We will refer to our frame elements as polynomial curvelets.

Let $\phi \in C^q([0, \infty))$, $q \in \mathbb{N}$, be a real-valued non-increasing function such that $\phi(t) = 1$ for $t \in [0, 1/2]$ and $\phi(t) = 0$ for $t \geq 1$. Then

$$\kappa(t) = \sqrt{\phi^2(t/2) - \phi^2(t)}, \quad 0 \leq t < \infty,$$

defines a window function $\kappa \in C^q([0, \infty))$ with $\text{supp}(\kappa) \subset [1/2, 2]$. In particular, it follows that

$$\sum_{j=1}^{\infty} \left| \kappa\left(\frac{n}{2^{j-1}}\right) \right|^2 = 1, \quad \text{for each } n \in \mathbb{N}. \quad (10)$$

Additionally, we consider directionality components of the form

$$\zeta_k^{d,n} = \frac{1}{\sqrt{2}} \begin{cases} 1, & \text{if } |k_{d-2}| = n, \\ 0, & \text{else,} \end{cases} \quad k = (k_1, \dots, k_{d-2}) \in \mathcal{I}_n^d, \quad n \in \mathbb{N}.$$

Clearly,

$$\sum_{k \in \mathcal{I}_n^d} |\zeta_k^{d,n}|^2 = 1, \quad \text{for each } n \in \mathbb{N}. \quad (11)$$

With the above defined window function κ and the directionality components $\zeta_k^{d,n}$, we now define an initial sequence $(\Psi^j)_{j=0}^\infty$ of polynomial curvelets via

$$\Psi^0 \equiv 1, \quad \Psi^j = \sum_{n=0}^\infty \sum_{k \in \mathcal{I}_n^d} \sqrt{\dim \mathcal{H}_n^d} \kappa\left(\frac{n}{2^{j-1}}\right) \zeta_k^{d,n} Y_k^{d,n}, \quad j \in \mathbb{N}. \quad (12)$$

We note that in the two-dimensional setting, i.e., for $d = 3$, this construction yields (essentially) the second-generation curvelets from [9].

By definition of the spherical harmonics given in (4), we have

$$Y_{(n, \dots, n, \pm n)}^{d,n}(x) = A_{(n, \dots, n)}^n(x_2 \pm ix_1)^n, \quad \text{for } x = (x_1, x_2, \dots, x_d) \in \mathbb{S}^{d-1}.$$

Thus, the polynomial curvelets defined above can be written as

$$\begin{aligned} \Psi^j(x) &= \sqrt{2} \sum_{n=0}^\infty \sqrt{\dim \mathcal{H}_n^d} \kappa\left(\frac{n}{2^{j-1}}\right) A_{(n, \dots, n)}^n \Re\{(x_2 + ix_1)^n\} \\ &= \sqrt{2} \sum_{n=0}^\infty \sqrt{\dim \mathcal{H}_n^d} \kappa\left(\frac{n}{2^{j-1}}\right) A_{(n, \dots, n)}^n |x_2 + ix_1|^n \cos(n \operatorname{Arg}(x_2 + ix_1)), \quad j \in \mathbb{N}. \end{aligned}$$

Here, $\Re\{z\}$ and $\operatorname{Arg}(z)$ denote the real part and the principal argument of $z \in \mathbb{C}$, respectively. To be precise, if $z \neq 0$ then $\operatorname{Arg}(z)$ is the unique element in $(-\pi, \pi]$ such that $z = |z| \exp(i \operatorname{Arg}(z))$. From this explicit representation, it is obvious that, at large scales j , the functions Ψ^j are well localized at e^2 . However, as mentioned in the two-dimensional setting [9], one might prefer to work with an initial sequence where each element is concentrated at the North Pole e^d . Hence, for an arbitrary rotation matrix $g_0 \in SO(d)$ with $g_0 e^1 = e^{d-1}$ and $g_0 e^2 = e^d$, we consider the rotated sequence $(\Psi_C^j)_{j=0}^\infty \subset \Pi(\mathbb{S}^{d-1})$, where

$$\Psi_C^j = T^d(g_0) \Psi^j, \quad j \in \mathbb{N}_0. \quad (13)$$

Clearly, the polynomial curvelets Ψ_C^j satisfy

$$\begin{aligned} \Psi_C^j(x) &= \sqrt{2} \sum_{n=0}^\infty \sqrt{\dim \mathcal{H}_n^d} \kappa\left(\frac{n}{2^{j-1}}\right) A_{(n, \dots, n)}^n \Re\{(x_d + ix_{d-1})^n\} \\ &= \sqrt{2} \sum_{n=0}^\infty \sqrt{\dim \mathcal{H}_n^d} \kappa\left(\frac{n}{2^{j-1}}\right) A_{(n, \dots, n)}^n |x_d + ix_{d-1}|^n \cos(n \operatorname{Arg}(x_d + ix_{d-1})), \quad (14) \end{aligned}$$

which implies that each Ψ_C^j is concentrated at e^d , where the localization increases with j . Moreover, (14) shows that

$$T^d(h) \Psi_C^j = \Psi_C^j, \quad \text{for each } h \in SO(d-2),$$

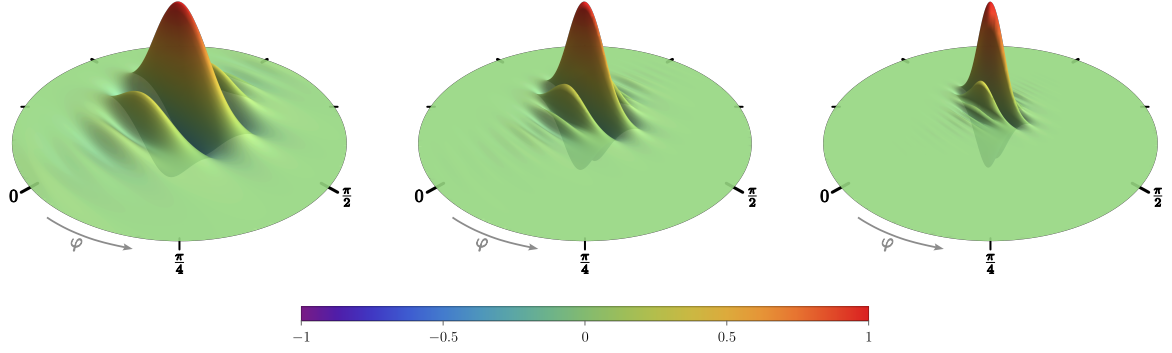


Figure 1: Re-scaled polynomial curvelets $\psi_C^j(t, \varphi)$, $(t, \varphi) \in [0, 1] \times [0, 2\pi)$, for $j = 5, 6, 7$ from left to right

as $\Psi_C^j(x_1, x_2, \dots, x_d)$ only depends on x_{d-1} and x_d . In the terminology of [14], the sequence $(\Psi_C^j)_{j=0}^\infty$ is $SO(d-2)$ -invariant. Hence, as discussed in [14], we can illustrate our polynomial curvelets in terms of the functions

$$\psi_C^j(t, \varphi) = \Psi_C^j(\cos t e^d + \sin t(\cos \varphi e^{d-1} + \sin \varphi(0, 0, \eta))), \quad (t, \varphi) \in [0, \pi] \times [0, 2\pi), \quad (15)$$

which are independent of $\eta \in \mathbb{S}^{d-3}$. For $\varphi \in [0, 2\pi)$, the map $t \mapsto \psi_C^j(t, \varphi)$ represents the function Ψ_C^j along the geodesic (unit-speed) curve $v: [0, \pi] \mapsto \mathbb{S}^{d-1}$ with $v(0) = e^d$, $v(\pi) = -e^d$, and $v'(0) = \cos \varphi e^{d-1} + \sin \varphi(0, 0, \eta)$. In particular, since the expression on the right-hand side of (15) does not depend on η , polynomial curvelets Ψ_C^j exhibit the same behavior along each of those paths $t \mapsto v(t)$, as long as φ is fixed. Consequently, we can replace $(0, 0, \eta)$ with e^{d-2} in (15).

In Figure 1 the functions ψ_C^j are visualized for $d = 4$, i.e., in the case where $\Psi_C^j \in \Pi_{2j}(\mathbb{S}^3)$, where we chose κ to be the C^∞ window function with $\text{supp}(\kappa) = [1/2, 2]$ defined in [16]. Here, for the sake of clarity, each of the images has been re-scaled to only take values in $[-1, 1]$. In addition to being well localized at the North Pole e^d , we observe that the curvelets Ψ_C^j decay fastest along the directions $\pm e^{d-1}$, which correspond to $\varphi \in \{0, \pi\}$ in Figure 1, and slowest in the directions $(0, 0, \eta'')$, $\eta'' \in \mathbb{S}^{d-3}$, which correspond to $\varphi \in \{\pi/2, 3\pi/2\}$.

Following the general approach from [14], the sequence $(\Psi_C^j)_{j=0}^\infty \subset \Pi(\mathbb{S}^{d-1})$ can be used to generate frames for $L^2(\mathbb{S}^{d-1})$ as follows. For each $j \in \mathbb{N}$, we require positive quadrature formulas of the form

$$\int_{\mathbb{S}^{d-1}} f d\omega_{d-1} = \sum_{r=1}^{r_j} \omega_{j,r} f(\eta_{j,r}), \quad \text{if } f \in \Pi_{2j+1}(\mathbb{S}^{d-1}), \quad (16)$$

and

$$\int_{\mathbb{S}^{d-2}} f d\omega_{d-2} = \sum_{s=1}^{s_j} \omega'_{j,s} f(\eta'_{j,s}), \quad \text{if } f \in \Pi_{2j+1}(\mathbb{S}^{d-2}), \quad (17)$$

with points $\eta_{j,r} \in \mathbb{S}^{d-1}$, $\eta'_{j,s} \in \mathbb{S}^{d-2}$ and corresponding weights $\omega_{j,r}, \omega'_{j,s} > 0$. For details on spherical quadrature rules and their construction, see [4, 5, 6, 12, 21, 25] and the references therein. In particular, we can assume (see e.g. [21]) that the numbers of samples in (16) and (17) satisfy

$$r_j \sim 2^{j(d-1)}, \quad s_j \sim 2^{j(d-2)}. \quad (18)$$

As suggested in [14, Section 4.5.3] for the setting of $SO(d-2)$ -invariant sequences, we consider the system

$$\mathcal{X}[(\Psi_C^j)_{j=0}^\infty] = \left\{ \sqrt{\omega_{j,r}\omega'_{j,s}} T^d(g_{\eta_{j,r}} h_{\eta'_{j,s}}) \Psi_C^j, \quad r = 1, \dots, r_j, \quad s = 1, \dots, s_j, \quad j \in \mathbb{N}_0 \right\}, \quad (19)$$

where $r_0 = s_0 = 1$, and where $\eta_{0,1} \in \mathbb{S}^{d-1}$, $\eta'_{0,1} \in \mathbb{S}^{d-2}$ can be chosen arbitrarily. Here, using the shorthand notation

$$\Psi_C^{j,r,s} = \sqrt{\omega_{j,r}\omega'_{j,s}} T^d(g_{\eta_{j,r}} h_{\eta'_{j,s}}) \Psi_C^j, \quad r = 1, \dots, r_j, \quad s = 1, \dots, s_j, \quad j \in \mathbb{N}_0,$$

we identify $\mathcal{X}[(\Psi_C^j)_{j=0}^\infty]$ with the (canonically) ordered sequence

$$(\Psi_C^{0,1,1}, \Psi_C^{1,1,1}, \dots, \Psi_C^{1,1,s_1}, \Psi_C^{1,2,1}, \dots, \Psi_C^{1,2,s_1}, \dots, \Psi_C^{1,r_1,s_1}, \Psi_C^{2,1,1}, \dots).$$

We note that, according to (18), the number of rotations at each scale j in (19) grows like $2^{j(2d-3)}$. In comparison, for previous constructions such as spherical needlets and directional polynomial wavelets, this number typically scales like $2^{j(d-1)}$, which can be regarded as a manifestation of their limited directional sensitivity (see [14] for more details).

Proposition 3.1

The system $\mathcal{X}[(\Psi_C^j)_{j=0}^\infty]$ is a Parseval frame for $L^2(\mathbb{S}^{d-1})$. In particular,

$$f = \sum_{j=0}^{\infty} \sum_{r=1}^{r_j} \sum_{s=1}^{s_j} \langle f, \Psi_C^{j,r,s} \rangle_{\mathbb{S}^{d-1}} \Psi_C^{j,r,s}$$

converges unconditionally in $L^2(\mathbb{S}^{d-1})$, for each $f \in L^2(\mathbb{S}^{d-1})$.

Proof. According to [14, Proposition 3.1] it suffices to show that

$$\delta_{n,0} + (\dim \mathcal{H}_n^d)^{-1} \sum_{j=1}^{\infty} \sum_{k \in \mathcal{I}_n^d} |\Psi_C^j(n, k)|^2 = 1, \quad \text{for each } n \in \mathbb{N}_0. \quad (20)$$

By construction, we have $\Psi_C^j = T^d(g_0) \Psi^j$, $j \in \mathbb{N}_0$, where Ψ^j is defined by (12). Therefore, $\Psi^j(n, k)$ and $\Psi_C^j(n, k) = \langle \Psi^j, T^d(g_0^{-1}) Y_k^{d,n} \rangle_{\mathbb{S}^{d-1}}$ both represent Fourier coefficients of Ψ^j w.r.t. the orthonormal bases $\{Y_k^{d,n}, k \in \mathcal{I}_n^d\}$ and $\{T^d(g_0^{-1}) Y_k^{d,n}, k \in \mathcal{I}_n^d\}$ of \mathcal{H}_n^d . Consequently,

$$\sum_{k \in \mathcal{I}_n^d} |\Psi_C^j(n, k)|^2 = \sum_{k \in \mathcal{I}_n^d} |\Psi^j(n, k)|^2$$

and thus (20) reduces to

$$\delta_{n,0} + \sum_{j=1}^{\infty} \left| \kappa \left(\frac{n}{2^{j-1}} \right) \right|^2 \sum_{k \in \mathcal{I}_n^d} |\zeta_k^{d,n}|^2 = 1, \quad \text{for each } n \in \mathbb{N}_0.$$

The assertion now follows easily from (10) and (11). \square

To conclude this section, we note that the curvelet expansion converges fast in the spaces $L^p(\mathbb{S}^{d-1})$, $1 \leq p \leq \infty$, where we recall that, by our convention, the symbol $L^\infty(\mathbb{S}^{d-1})$ refers to the Banach space of continuous functions on \mathbb{S}^{d-1} . For each $J \in \mathbb{N}_0$, let $\Lambda_J: L^1(\mathbb{S}^{d-1}) \rightarrow \Pi_{2^J}(\mathbb{S}^{d-1})$ be the linear operator defined by

$$\Lambda_J f = \sum_{j=0}^J \sum_{r=1}^{r_j} \sum_{s=1}^{s_j} \langle f, \Psi_C^{j,r,s} \rangle_{\mathbb{S}^{d-1}} \Psi_C^{j,r,s}.$$

Also, let

$$E_m(f)_p = \inf_{P \in \Pi_m(\mathbb{S}^{d-1})} \|f - P\|_{L^p(\mathbb{S}^{d-1})}, \quad m \in \mathbb{N}_0, \quad 1 \leq p \leq \infty,$$

denote the error of the best approximation of $f \in L^p(\mathbb{S}^{d-1})$ in $\Pi_m(\mathbb{S}^{d-1})$ w.r.t. $\|\cdot\|_{L^p(\mathbb{S}^{d-1})}$. Then we have the following result, where we assume, for the sake of simplicity, that the function ϕ utilized in the beginning of the section is infinitely often differentiable, i.e., $\phi \in C^\infty([0, \infty))$.

Proposition 3.2

Let $1 \leq p \leq \infty$. Then

$$\|f - \Lambda_J f\|_{L^p(\mathbb{S}^{d-1})} \leq c_p E_{2^{J-1}}(f)_p, \quad \text{for each } f \in L^p(\mathbb{S}^{d-1}).$$

Proof. Exactly as in the proof of [30, Lemma 5.1], a simple calculation shows that

$$\Lambda_J f = \sum_{n=0}^{\infty} \sum_{k \in \mathcal{I}_n^d} \phi^2\left(\frac{n}{2^J}\right) \langle f, Y_k^{d,n} \rangle_{\mathbb{S}^{d-1}} Y_k^{d,n}.$$

In other words, $\Lambda_J f = f * \Phi^J$, where

$$f * \Phi^J(\eta) = \langle f, T^d(g_\eta) \Phi^J \rangle_{\mathbb{S}^{d-1}}, \quad \eta \in \mathbb{S}^{d-1},$$

denotes the standard spherical convolution of f with the zonal scaling function

$$\Phi^J = \sum_{n=0}^{\infty} \sum_{k \in \mathcal{I}_n^d} \phi^2\left(\frac{n}{2^J}\right) \overline{Y_k^{d,n}(e^d)} Y_k^{d,n}. \quad (21)$$

For such a kernel (21), it is well known that $\|f * \Phi^J\|_{L^p(\mathbb{S}^{d-1})} \leq c_p \|f\|_{L^p(\mathbb{S}^{d-1})}$. A proof of the latter can be found in [11, Theorem 2.6.3].

It is easy to see that $\Lambda_J f = f$ for each $f \in \Pi_{2^{J-1}}(\mathbb{S}^{d-1})$. Thus, if $P \in \Pi_{2^{J-1}}(\mathbb{S}^{d-1})$ is the best approximation of f in $\Pi_{2^{J-1}}(\mathbb{S}^{d-1})$ w.r.t. $\|\cdot\|_{L^p(\mathbb{S}^{d-1})}$, then

$$\|f - \Lambda_J f\|_{L^p(\mathbb{S}^{d-1})} \leq \|f - P\|_{L^p(\mathbb{S}^{d-1})} + \|\Lambda_J(P - f)\|_{L^p(\mathbb{S}^{d-1})} \leq c_p E_{2^{J-1}}(f)_p.$$

□

4 Localization

In the following, we derive a localization bound for polynomial curvelets. Here, in contrast to the established estimates (1) for spherical needlets [7, 11, 25, 26] and directional polynomial wavelets [30, 31], the upper bound exhibits a direction-dependent decay, which indicates a particularly strong directional sensitivity. We note that, for $d = 3$, where our frames essentially coincide with the second-generation curvelets from [9], the following localization estimate was previously established in [29, Proposition 2.4].

Theorem 4.1

Let $\Psi_{\mathbb{C}}^j$, $j \in \mathbb{N}_0$, be as defined in Section 3 with $\kappa \in C^q([0, \infty))$ for some $q \in \mathbb{N}$. We assume that there exists some $t_0 \in (1/2, 2)$ such that $\kappa^{(q)}(t) \neq 0$ for each $t \in (1/2, t_0)$. Then

$$|\Psi_{\mathbb{C}}^j(x)| \leq \frac{c_q 2^{j(3d-2)/4} |x_d + ix_{d-1}|^{2^{j-2}}}{(1 + 2^j |\text{Arg}(x_d + ix_{d-1})|)^q}, \quad x = (x_1, \dots, x_d) \in \mathbb{S}^{d-1}.$$

Here, $c_q > 0$ is a constant which only depends on κ, q , and d .

Proof. Our proof uses arguments similar to those in the two-dimensional setting [29, Proposition 2.4]. We start from the representation given in (14), i.e.,

$$\Psi_{\mathbb{C}}^j(x) = \sqrt{2} \sum_{n=0}^{\infty} \sqrt{\dim \mathcal{H}_n^d} \kappa\left(\frac{n}{2^{j-1}}\right) A_{(n, \dots, n)}^n |x_d + ix_{d-1}|^n \cos(n \text{Arg}(x_d + ix_{d-1})).$$

Utilizing the duplication formula for the Gamma function, the normalization constants $A_{(n, \dots, n)}^n$ defined by (5) can be written in the form

$$A_{(n, \dots, n)}^n = \frac{2^{(2-d)/2}}{\sqrt{\Gamma(\frac{d}{2})}} \prod_{j=0}^{d-3} \sqrt{\frac{(2n + d - j - 2)\Gamma(n + \frac{d-j-2}{2})}{\Gamma(n + \frac{d-j-1}{2})}}. \quad (22)$$

With (6) and (22), it is easy to verify that there exist constants c_0, c_1, \dots, c_{q-1} such that

$$\sqrt{\dim \mathcal{H}_n^d} A_{(n, \dots, n)}^n = n^{3(d-2)/4} \left(\sum_{p=0}^{q-1} c_p n^{-p} + \mathcal{O}(n^{-q}) \right), \quad n \rightarrow \infty.$$

Consequently,

$$\Psi_{\mathbb{C}}^j(x) = R_j(x) + \sum_{p=0}^{q-1} c_p \sum_{n=0}^{\infty} \kappa\left(\frac{n}{2^{j-1}}\right) n^{3(d-2)/4-p} |x_d + ix_{d-1}|^n \cos(n \text{Arg}(x_d + ix_{d-1}))$$

where, due to the fact that $\text{supp}(\kappa) \subset [1/2, 2]$,

$$|R_j(x)| \leq c_q 2^{j((3d-2)/4-q)} |x_d + ix_{d-1}|^{2^{j-2}}.$$

To complete the proof, it suffices to show that

$$\left| \sum_{n=0}^{\infty} \kappa\left(\frac{n}{N}\right) n^{3(d-2)/4-p} z^n \cos(n\varphi) \right| \leq \frac{c_p z^{N/2} N^{(3d-2)/4}}{(1 + N\varphi)^q},$$

for each $N \in \mathbb{N}$, $z \in [0, 1]$, and $\varphi \in [0, \pi]$. In order to do so, we first observe that

$$\kappa\left(\frac{n}{N}\right) n^{3(d-2)/4-p} z^n = N^{3(d-2)/4-p} h_{z,N}\left(\frac{n}{N}\right),$$

with $h_{z,N}(t) = \kappa(t) t^{3(d-2)/4-p} z^{Nt}$. Clearly, $h_{z,N} \in C^q([0, \infty))$ with $\text{supp}(h_{z,N}) \subset [1/2, 2]$. Thus, it suffices to prove the estimate

$$\left| \frac{1}{N} \sum_{n=0}^{\infty} h_{z,N}\left(\frac{n}{N}\right) \cos(n\varphi) \right| \leq \frac{c_q z^{N/2}}{(1 + N\varphi)^q}. \quad (23)$$

Applying [22, Lemma 5], we have

$$\left| \frac{1}{N} \sum_{n=0}^{\infty} h_{z,N}\left(\frac{n}{N}\right) \cos(n\varphi) \right| \leq \left| \int_0^2 h_{z,N}(t) \cos(Nt\varphi) dt \right| + \frac{c_q V(h_{z,N}^{(q-1)})}{N^q}, \quad (24)$$

where

$$V(h_{z,N}^{(q-1)}) = \int_0^2 |h_{z,N}^{(q)}(t)| dt, \quad h_{z,N}^{(q)}(t) = \frac{d^q}{dt^q} h_{z,N}(t).$$

Here, $V(h_{z,N}^{(q-1)}) \leq c_q z^{N/2}$, which can be verified as follows. By Leibniz's rule, $h_{z,N}^{(q)}(t)$ is a linear combination of functions of the form

$$\kappa^{(q-\ell)}(t) \frac{d^{\ell-k}}{dt^{\ell-k}} \left(t^{3(d-2)/4-p} (\ln z^N)^k z^{Nt} \right), \quad 0 \leq k \leq \ell \leq q.$$

Thus, it is sufficient to prove the estimate

$$|\ln(z^N)|^k \int_{1/2}^2 z^{Nt} |\kappa^{(q-\ell)}(t)| dt \leq c_q z^{N/2}. \quad (25)$$

By definition of κ , we have $\kappa^{(m)}(1/2) = \kappa^{(m)}(2) = 0$ for $0 \leq m \leq q$. Also, by assumption there exists some $t_0 \in (1/2, 2)$ such that $\kappa^{(q)}$ does not vanish in $(1/2, t_0)$. Hence, the mean value theorem implies that $\kappa^{(m)}(t) \neq 0$, for all $t \in (1/2, t_0)$, $0 \leq m \leq q$. It follows that

$$\int_{1/2}^2 z^{Nt} |\kappa^{(q-\ell)}(t)| dt = \left| \int_{1/2}^{t_0} z^{Nt} \kappa^{(q-\ell)}(t) dt \right| + \int_{t_0}^2 z^{Nt} |\kappa^{(q-\ell)}(t)| dt.$$

Repeated integration by parts yields

$$\int_{1/2}^{t_0} z^{Nt} \kappa^{(q-\ell)}(t) dt = z^{Nt_0} \sum_{r=0}^{k-1} \frac{\kappa^{(q-\ell+1)}(t_0)}{(\ln z^N)^{r+1}} + \frac{(-1)^k}{(\ln z^N)^k} \int_{1/2}^{t_0} z^{Nt} \kappa^{(q-\ell+k)}(t) dt.$$

Thus, since $s^\delta \ln(s)^m \rightarrow 0$ as $s \rightarrow 0^+$, for all $\delta > 0$ and all $m \in \mathbb{N}$, it is now easy to see that (25) holds. Consequently, $V(h_{z,N}^{(q-1)}) \leq c_q z^{N/2}$, as claimed. Indeed, by the same argument we find that $V(h_{z,N}^{(m)}) \leq c_q z^{N/2}$, for each $0 \leq m \leq q-1$.

Lastly, we derive an estimate for the integral on the right hand side of (24). Here, applying integration by parts repeatedly and using the fact that $V(h_{z,N}^{(m)}) \leq c_q z^{N/2}$, for

$0 \leq m \leq q - 1$, we obtain

$$\begin{aligned} \left| \int_0^2 h_{z,N}(t) \cos(Nt\varphi) dt \right| &\leq \left| \int_0^2 h_{z,N}(t) e^{iNt\varphi} dt \right| \\ &= \left| \int_0^2 h_{z,N}(t) e^{-it} e^{it(1+N\varphi)} dt \right| \\ &\leq \frac{c_q z^{N/2}}{(1+N\varphi)^q}. \end{aligned}$$

This completes the proof. \square

[Theorem 4.1](#) can be utilized to study the behavior of $\|\Psi_C^j\|_{L^p(\mathbb{S}^{d-1})}$ as j becomes large. Precisely, we have the following result.

Corollary 4.2

Let Ψ_C^j , $j \in \mathbb{N}_0$, be as defined in [Section 3](#), with the same assumptions on $\kappa \in C^q([0, \infty))$ as in [Theorem 4.1](#). If $0 < p < \infty$ and $q > 1/p$, then

$$\|\Psi_C^j\|_{L^p(\mathbb{S}^{d-1})} \sim 2^{j((3d-2)/4 - d/(2p))}.$$

Moreover, (as long as $q \geq 1$) it holds that

$$\|\Psi_C^j\|_{L^\infty(\mathbb{S}^{d-1})} = |\Psi_C^j(e^d)| \sim 2^{j(3d-2)/4}.$$

Here, the constants of equivalence only depend on κ, q, p , and d .

Proof. We closely follow the arguments for the zonal setting given in [\[24\]](#). In some instances, it will be convenient to work with the functions $\Psi^j = T(g_0^{-1})\Psi_C^j$ given by [\(12\)](#), rather than with the curvelets Ψ_C^j themselves. Of course, the latter does not pose any problems due to the rotational invariance of the surface measure ω_{d-1} on \mathbb{S}^{d-1} .

For $p = 2$, the representation [\(12\)](#) immediately yields

$$\|\Psi^j\|_{L^2(\mathbb{S}^{d-1})}^2 = \sum_{n=0}^{\infty} \dim \mathcal{H}_n^d \left| \kappa\left(\frac{n}{2^{j-1}}\right) \right|^2.$$

Thus, using [\(6\)](#), it is not difficult to verify that $\|\Psi^j\|_{L^2(\mathbb{S}^{d-1})} \sim 2^{j(d-1)/2}$.

In the general case $p \in (0, \infty)$, we can utilize [Theorem 4.1](#), which, in terms of spherical coordinates [\(3\)](#), implies the estimate

$$|\Psi^j(\theta_1, \dots, \theta_{d-1})| \leq \frac{c_q \left(\prod_{m=2}^{d-1} \sin \theta_m \right)^{2^{j-2}} 2^{j(3d-2)/4}}{(1 + 2^j |\theta_1|)^q}.$$

With this estimate, a straightforward calculation yields

$$\|\Psi^j\|_{L^p(\mathbb{S}^{d-1})}^p \leq c_q 2^{j(p(3d-2)/4 - 1)} \left(\int_0^{\pi/2} (\sin \theta)^{2^{j-2}p} d\theta \right)^{d-2},$$

provided that $q > 1/p$. By the well-known formula

$$\int_0^{\pi/2} \sin^m \theta d\theta = \frac{\sqrt{\pi} \Gamma(\frac{m+1}{2})}{2\Gamma(\frac{m+2}{2})} \leq cm^{-1/2},$$

it now follows that

$$\|\Psi^j\|_{L^p(\mathbb{S}^{d-1})} \leq c2^{j((3d-2)/4-d/(2p))}.$$

The estimate $\|\Psi_C^j\|_{L^\infty(\mathbb{S}^{d-1})} = |\Psi_C^j(e^d)| \leq c2^{j(3d-2)/4}$ is a direct consequence of (14) and Theorem 4.1. It can be used to obtain the corresponding lower bound in the case $0 < p < 2$, since

$$\|\Psi_C^j\|_{L^2(\mathbb{S}^{d-1})}^2 \leq \|\Psi_C^j\|_{L^\infty(\mathbb{S}^{d-1})}^{2-p} \|\Psi_C^j\|_{L^p(\mathbb{S}^{d-1})}^p.$$

For $2 < p \leq \infty$, the lower estimate follows from the above and from Hölder's inequality. Precisely, we have

$$\|\Psi_C^j\|_{L^2(\mathbb{S}^{d-1})}^2 \leq \|\Psi_C^j\|_{L^p(\mathbb{S}^{d-1})} \|\Psi_C^j\|_{L^q(\mathbb{S}^{d-1})}, \quad q = \frac{p}{p-1},$$

as well as

$$\|\Psi_C^j\|_{L^2(\mathbb{S}^{d-1})}^2 \leq \|\Psi_C^j\|_{L^\infty(\mathbb{S}^{d-1})} \|\Psi_C^j\|_{L^1(\mathbb{S}^{d-1})}.$$

This completes the proof. \square

We note that the asymptotic behavior

$$\|\Psi_C^j\|_{L^p(\mathbb{S}^{d-1})} \sim 2^{j((3d-2)/4-d/(2p))}, \quad 0 < p \leq \infty, \quad (26)$$

established in Corollary 4.2, deviates from the typical scaling of the L^p -norms for previously considered polynomial frames. Specifically, if $(\tilde{\Psi}^j)_{j=0}^\infty$ represents an initial sequence of spherical needlets or directional polynomial wavelets on \mathbb{S}^{d-1} , then, according to [24] and [30],

$$\|\tilde{\Psi}^j\|_{L^p(\mathbb{S}^{d-1})} \sim 2^{j(d-1)(1-1/p)}, \quad 0 < p \leq \infty. \quad (27)$$

Clearly, (26) and (27) only coincide in the case $p = 2$.

5 Directional sensitivity

For the moment, let $(\Psi^j)_{j=0}^\infty$ be an arbitrary sequence of spherical polynomials $\Psi^j \in \Pi_{2j}(\mathbb{S}^{d-1})$. We assume that each of these polynomials is (in some sense) concentrated at the North Pole e^d . In this setting, the functions

$$T^d(h)\Psi^j, \quad h \in SO(d-1),$$

are also concentrated at e^d , and we refer to them as orientations of Ψ^j . As proposed in the two-dimensional setting [35], the directionality of Ψ^j can be measured using the auto-correlation function

$$SO(d-1) \rightarrow \mathbb{C}, \quad h \mapsto \langle T^d(h)\Psi^j, \Psi^j \rangle_{\mathbb{S}^{d-1}},$$

which tests Ψ^j against its various orientations. In this context, a high directional sensitivity of Ψ^j is associated with an auto-correlation function that is well localized at the identity matrix $I_d \in SO(d-1)$.

Previous constructions of localized polynomial frames generated by an initial sequence $(\Psi^j)_{j=0}^\infty$, namely spherical needlets [1, 10, 11, 13, 18, 19, 20, 22, 24, 25, 26], directional wavelets [16, 17, 30, 35], and second-generation curvelets [9, 29], differ vastly in their degree

of directionality. Specifically, if $(\Psi_N^j)_{j=0}^\infty$ denotes an initial sequence of spherical needlets, then

$$\langle T^d(h)\Psi_N^j, \Psi_N^j \rangle_{\mathbb{S}^{d-1}} = \|\Psi_N^j\|_{L^2(\mathbb{S}^{d-1})}^2, \quad \text{for each } h \in SO(d-1).$$

Hence, the corresponding auto-correlation functions are constant and the associated frames do not exhibit any directionality whatsoever. If $(\Psi_{W,K}^j)_{j=0}^\infty$ denotes an initial sequence of directional wavelets on \mathbb{S}^2 , as defined in [16, 35], where $K \in \mathbb{N}_0$ is some fixed parameter controlling the degree of anisotropy, then

$$\langle T^3(h(\gamma))\Psi_{W,K}^j, \Psi_{W,K}^j \rangle_{\mathbb{S}^2} = \sum_{n=0}^{\infty} \dim \mathcal{H}_n^3 \left| \kappa\left(\frac{n}{2^{j-1}}\right) \right|^2 \cos^{K_n} \gamma, \quad \gamma \in [0, 2\pi), \quad (28)$$

in which $K_n = \min(K, n)$ and $h(\gamma) \in \mathbb{R}^{3 \times 3}$ is a positive rotation by γ in the (x_1, x_2) -plane. Recently, we introduced directional polynomial wavelets $\Psi_{W,K}^j \in \Pi_{2^j}(\mathbb{S}^{d-1})$ for higher-dimensional spheres (see [30]). Here, we have shown that

$$\langle T^d(h)\Psi_{W,K}^j, \Psi_{W,K}^j \rangle_{\mathbb{S}^{d-1}} = \sum_{n=0}^{\infty} \dim \mathcal{H}_n^d \left| \kappa\left(\frac{n}{2^{j-1}}\right) \right|^2 (\langle e^{d-1}, h e^{d-1} \rangle)^{K_n}, \quad h \in SO(d-1). \quad (29)$$

The formulas (28) and (29) imply that, in contrast to spherical needlets, directional polynomial wavelets can exhibit a strong degree of directional sensitivity, provided that K is chosen large enough. However, since K is a parameter that must be fixed a priori, the directionality does not increase with j . Frames with this property are also referred to as steerable frames (see [14, 16, 17, 30, 34, 35]).

Among the previously considered constructions of localized polynomial frames, second-generation curvelets on \mathbb{S}^2 , as introduced in [9], stand out because they are unlimited in their directional resolution. Indeed, this property carries over to the higher-dimensional polynomial curvelets defined in Section 3. Specifically, we have the following result.

Proposition 5.1

Let Ψ_C^j be as defined in Section 3. For $d = 3$,

$$\langle T^3(h(\gamma))\Psi_C^j, \Psi_C^j \rangle_{\mathbb{S}^2} = \sum_{n=0}^{\infty} \dim \mathcal{H}_n^3 \left| \kappa\left(\frac{n}{2^{j-1}}\right) \right|^2 \left(\cos^{2n} \frac{\gamma}{2} + \sin^{2n} \frac{\gamma}{2} \right), \quad \gamma \in [0, 2\pi), \quad (30)$$

where $h(\gamma) \in \mathbb{R}^{3 \times 3}$ is a positive rotation by γ in the (x_1, x_2) -plane. If $d \geq 4$, then

$$\begin{aligned} & \langle T^d(h)\Psi_C^j, \Psi_C^j \rangle_{\mathbb{S}^{d-1}} \\ &= 2 \sum_{n=0}^{\infty} \dim \mathcal{H}_n^d \left| \kappa\left(\frac{n}{2^{j-1}}\right) \right|^2 \sum_{\substack{m=0 \\ m \text{ even}}}^n |c(d, n, m)|^2 \frac{\Gamma(d-3)m!}{\Gamma(m+d-3)} C_m^{\frac{d-3}{2}} (\langle h e^{d-1}, e^{d-1} \rangle), \end{aligned} \quad (31)$$

for each $h \in SO(d-1)$, where

$$c(d, n, m) = A_{(m,0,\dots,0)}^n A_{(n,\dots,n)}^n \frac{\sqrt{\pi} \Gamma(\frac{d}{2}) \binom{n}{m} \Gamma(m+d-3) (-i)^m}{2^{m+d-4} (n + \frac{d-2}{2}) \Gamma(\frac{d-2}{2}) \Gamma(\frac{d-3}{2}) \Gamma(m + \frac{d-2}{2})}.$$

Proof. For $d = 3$, the analysis functions Ψ_C^j (essentially) coincide with the second-generation curvelets from [9], and (30) follows from [29, Proposition 2.3].

Now, we consider the case $d \geq 4$. The following proof relies on fundamental properties of the matrix functions associated with the unitary group representation T^d . These properties are summarized in the [Appendix](#) of this article. By (13), we have

$$\Psi_C^j = \frac{1}{\sqrt{2}} \sum_{n=0}^{\infty} \sqrt{\dim \mathcal{H}_n^d} \kappa\left(\frac{n}{2^{j-1}}\right) \left(T^d(g_0) Y_{(n,\dots,n)}^{d,n} + T^d(g_0) Y_{(n,\dots,n)^-}^{d,n} \right),$$

with $(n, \dots, n, n)^- = (n, \dots, n, -n)$. Hence, it follows from the definition of the matrix functions in (A.2) that

$$\langle T^d(h) \Psi_C^j, \Psi_C^j \rangle_{\mathbb{S}^{d-1}} = \sum_{n=0}^{\infty} \dim \mathcal{H}_n^d \left| \kappa\left(\frac{n}{2^{j-1}}\right) \right|^2 L_n(h),$$

where

$$L_n(h) = \frac{1}{2} \left(t_{(n,\dots,n),(n,\dots,n)}^{d,n}(g_0^{-1} h g_0) + t_{(n,\dots,n)^-, (n,\dots,n)}^{d,n}(g_0^{-1} h g_0) \right. \\ \left. + t_{(n,\dots,n),(n,\dots,n)^-}^{d,n}(g_0^{-1} h g_0) + t_{(n,\dots,n)^-, (n,\dots,n)^-}^{d,n}(g_0^{-1} h g_0) \right). \quad (32)$$

Here, using (A.6) and (A.8), we obtain

$$t_{(n,\dots,n),(n,\dots,n)}^{d,n}(g_0^{-1} h g_0) = \sum_{m=0}^n \sum_{k,\ell \in \mathcal{I}_m^{d-1}} t_{(n,\dots,n),(m,k)}^{d,n}(g_0^{-1}) t_{k,\ell}^{d-1,m}(h) t_{(m,\ell),(n,\dots,n)}^{d,n}(g_0). \quad (33)$$

Similar expressions hold for the other matrix functions in (32).

Clearly, L_n is an element of the polynomial subspace $\mathcal{M}_n^1(SO(d-1))$ defined in (A.10). Also, by (14), Ψ_C^j is invariant under rotations that keep e^d and e^{d-1} fixed, i.e.,

$$T^d(k) \Psi_C^j = \Psi_C^j, \quad \text{for each } k \in SO(d-2). \quad (34)$$

Indeed, (34) is a direct consequence of the $SO(d-2)$ -invariance of the spherical harmonics $T^d(g_0) Y_{(n,\dots,n)}^{d,n}$ and $T^d(g_0) Y_{(n,\dots,n)^-}^{d,n}$. It follows that L_n exhibits the symmetry

$$L_n(k_1 h k_2) = L_n(h), \quad \text{for } k_1, k_2 \in SO(d-2), h \in SO(d-1). \quad (35)$$

The symmetry (35) implies that L_n is a linear combination of the matrix functions $t_{0,0}^{d-1,m}$, as we will now demonstrate. Let $m \in \mathbb{N}_0$ and $r, s \in \mathcal{I}_m^{d-1}$. By (A.1) and (A.6), we have

$$\langle L_n, t_{r,s}^{d-1,m} \rangle_{SO(d-1)} = \int_{\mathbb{S}^{d-2}} \int_{SO(d-2)} L_n(h_\eta k) \overline{t_{r,s}^{d-1,m}(h_\eta k)} d\mu_{d-2}(k) d\omega_{d-2}(\eta) \\ = \int_{\mathbb{S}^{d-2}} L_n(h_\eta) \int_{SO(d-2)} \sum_{q \in \mathcal{I}_m^{d-1}} \overline{t_{r,q}^{d-1,m}(h_\eta) t_{q,s}^{d-1,m}(k)} d\mu_{d-2}(k) d\omega_{d-2}(\eta).$$

According to (A.8), it holds that $t_{q,s}^{d-1,m}(k) = \delta_{q_1, s_1} t_{(q_2, \dots, q_{d-2}), (s_2, \dots, s_{d-2})}^{d-2, s_1}(k)$, for each $k \in SO(d-2)$ and $d \geq 5$. For $d = 4$, (A.9) yields $t_{q,s}^{3,m}(k(\gamma)) = \delta_{q,s} e^{iq\gamma}$, where $k(\gamma) \in \mathbb{R}^{3 \times 3}$ is a

positive rotation by γ in the (x_1, x_2) -plane. Thus, due to the orthogonality of the matrix functions and due to the fact that $t_{0,0}^{d-2,0} \equiv 1$, for $d \geq 5$, we obtain

$$\langle L_n, t_{r,s}^{d-1,m} \rangle_{SO(d-1)} = \delta_{s,0} \langle L_n, t_{r,0}^{d-1,m} \rangle_{SO(d-1)}.$$

At this point, we confirmed that L_n can be written as a linear combination of the matrix functions $t_{r,0}^{d-1,m}$, with $r \in \mathcal{I}_m^{d-1}$, $0 \leq m \leq n$. In particular, using (A.7), the function $F_n: \mathbb{S}^{d-2} \rightarrow \mathbb{C}$ defined by $F_n(\eta) = L_n(h_\eta)$ constitutes a polynomial of degree n on \mathbb{S}^{d-2} , i.e., $F_n \in \Pi_n(\mathbb{S}^{d-2})$. By (35),

$$F_n(k\eta) = L_n(kh_\eta) = L_n(h_\eta) = F_n(\eta), \quad \text{for each } k \in SO(d-2), \eta \in \mathbb{S}^{d-2}.$$

Since $Y_0^{d-1,m}$ is the unique element in \mathcal{H}_m^{d-1} , up to multiplication by a scalar, that is invariant under the group $SO(d-2)$ (see e.g. [11, Lemma 1.7.1]), it follows that

$$F_n = \sum_{m=0}^n \langle F_n, Y_0^{d-1,m} \rangle_{\mathbb{S}^{d-2}} Y_0^{d-1,m}.$$

Hence, by the relation $L_n(h) = F_n(he^{d-1})$ and by (A.7), we obtain

$$\langle L_n, t_{r,s}^{d-1,m} \rangle_{SO(d-1)} = \delta_{s,0} \delta_{r,0} \langle L_n, t_{0,0}^{d-1,m} \rangle_{SO(d-1)}. \quad (36)$$

Now, we consider the representation of L_n given in (32). By expanding the involved matrix functions as in (33), and by using (36), it follows that

$$\begin{aligned} L_n(h) &= \frac{1}{2} \sum_{m=0}^n t_{0,0}^{d-1,m}(h) \left(t_{(n,\dots,n),(m,0,\dots,0)}^{d,n}(g_0^{-1}) t_{(m,0,\dots,0),(n,\dots,n)}^{d,n}(g_0) \right. \\ &\quad + t_{(n,\dots,n)^-, (m,0,\dots,0)}^{d,n}(g_0^{-1}) t_{(m,0,\dots,0),(n,\dots,n)}^{d,n}(g_0) + t_{(n,\dots,n),(m,0,\dots,0)}^{d,n}(g_0^{-1}) t_{(m,0,\dots,0),(n,\dots,n)^-}^{d,n}(g_0) \\ &\quad \left. + t_{(n,\dots,n)^-, (m,0,\dots,0)}^{d,n}(g_0^{-1}) t_{(m,0,\dots,0),(n,\dots,n)^-}^{d,n}(g_0) \right). \end{aligned}$$

Moreover, the symmetries (A.3) and (A.4) yield

$$\begin{aligned} L_n(h) &= \frac{1}{2} \sum_{m=0}^n t_{0,0}^{d-1,m}(h) \left(\left| t_{(n,\dots,n),(m,0,\dots,0)}^{d,n}(g_0^{-1}) \right|^2 + \left| t_{(n,\dots,n)^-, (m,0,\dots,0)}^{d,n}(g_0^{-1}) \right|^2 \right. \\ &\quad \left. + 2\Re \left\{ \left(t_{(n,\dots,n)^-, (m,0,\dots,0)}^{d,n}(g_0^{-1}) \right)^2 \right\} \right). \end{aligned}$$

Here, using (A.7), it is not difficult to verify that

$$t_{0,0}^{d-1,m}(h) = \frac{\Gamma(d-3)m!}{\Gamma(m+d-3)} C_m^{\frac{d-3}{2}} (\langle he^{d-1}, e^{d-1} \rangle).$$

For an explicit reference of this formula, we refer to [32, p. 471].

In order to prove (31), it remains to show that

$$t_{(n,\dots,n),(m,0,\dots,0)}^{d,n}(g_0^{-1}) = c(d, n, m). \quad (37)$$

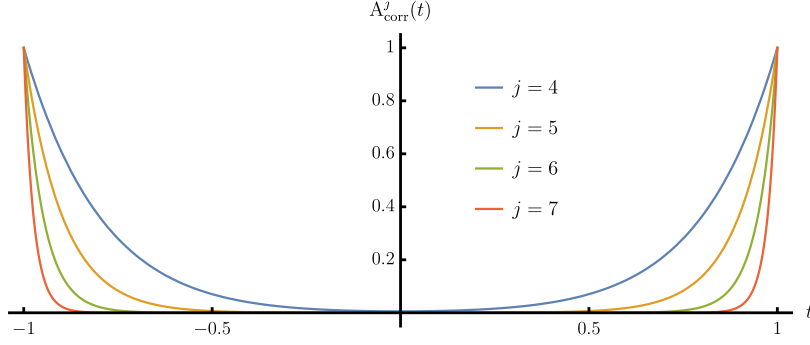


Figure 2: Auto-correlation function A_{corr}^j for $j = 4, 5, 6, 7$

We have

$$\begin{aligned}
t_{(n,\dots,n),(m,0,\dots,0)}^{d,n}(g_0^{-1}) &= \int_{\mathbb{S}^{d-1}} Y_{(m,0,\dots,0)}^{d,n}(x) \overline{T^d(g_0) Y_{(n,\dots,n)}^{d,n}(x)} d\omega_{d-1}(x) \\
&= A_{(m,0,\dots,0)}^n A_{(n,\dots,n)}^n \int_{\mathbb{S}^{d-1}} C_{n-m}^{\frac{d-2}{2}+m}(x_d) (1-x_d^2)^{m/2} \\
&\quad \times C_m^{\frac{d-3}{2}}\left(\frac{x_{d-1}}{\sqrt{1-x_d^2}}\right) (x_d - ix_{d-1})^n d\omega_{d-1}(x).
\end{aligned}$$

In terms of spherical coordinates (3),

$$\begin{aligned}
&\int_{\mathbb{S}^{d-1}} C_{n-m}^{\frac{d-2}{2}+m}(x_d) (1-x_d^2)^{m/2} C_m^{\frac{d-3}{2}}\left(\frac{x_{d-1}}{\sqrt{1-x_d^2}}\right) (x_d - ix_{d-1})^n d\omega_{d-1}(x) \\
&= c(d) \int_0^\pi C_{n-m}^{\frac{d-2}{2}+m}(\cos \theta_{d-1}) H_{n,m}(\theta_{d-1}) (\sin \theta_{d-1})^{m+d-2} d\theta_{d-1},
\end{aligned}$$

where $c(d) = \Gamma(\frac{d}{2}) / (\pi \Gamma(\frac{d-2}{2}))$ and

$$H_{n,m}(\theta_{d-1}) = \int_0^\pi C_m^{\frac{d-3}{2}}(\cos \theta_{d-1}) (\cos \theta_{d-1} - i \cos \theta_{d-2} \sin \theta_{d-1})^n \sin^{d-3} \theta_{d-2} d\theta_{d-2}.$$

A well-known representation formula for Gegenbauer polynomials (see e.g. [32, p. 483]) yields

$$H_{n,m}(\theta) = \frac{2^{m+1} \sqrt{\pi} \Gamma(\frac{d-2}{2} + m) n! \Gamma(m+d-3)}{m! \Gamma(\frac{d-3}{2}) \Gamma(n+m+d-2) i^m} \sin^m \theta C_{n-m}^{\frac{d-2}{2}+m}(\cos \theta).$$

Furthermore, as shown in [32, p. 462],

$$\int_0^\pi |C_{n-m}^{\frac{d-2}{2}+m}(\cos \theta)|^2 (\sin \theta)^{2m+d-2} d\theta = \frac{\pi \Gamma(n+m+d-2)}{2^{2m+d-3} (n-m)! (n+\frac{d-2}{2}) \Gamma^2(m+\frac{d-2}{2})}.$$

By combining all of the above, formula (37) can be verified, and thus the proof of (31) is complete. \square

In Figure 2, the normalized auto-correlation functions

$$A_{\text{corr}}^j(t) = \frac{\langle T^d(h) \Psi_C^j, \Psi_C^j \rangle_{\mathbb{S}^{d-1}}}{\|\Psi_C^j\|_{L^2(\mathbb{S}^{d-1})}^2}, \quad t = \langle h e^{d-1}, e^{d-1} \rangle,$$

are visualized for $d = 4$, i.e., in the case where $\Psi_C^j \in \Pi_{2j}(\mathbb{S}^3)$, and for different scales j . Here, the representation of $\langle T^d(h)\Psi_C^j, \Psi_C^j \rangle_{\mathbb{S}^{d-1}}$ as a function of $t = \langle he^{d-1}, e^{d-1} \rangle$ is given by (31) and we chose κ to be the C^∞ window with $\text{supp}(\kappa) = [1/2, 2]$ constructed in [16].

6 Detection of singularities

To conclude this article, we demonstrate the potential of polynomial curvelets for applications that require localized analyses of anisotropic features. Here, we focus on the problem of identifying edges and higher-order singularities by the asymptotic decay of the curvelet coefficients. Specifically, we will derive a higher-dimensional version of a previous result for the two-dimensional setting [29, Theorem 3.3].

For $z \in \mathbb{S}^{d-1}$, $r \in (0, \pi)$, and $\tau \in \mathbb{N}_0$, we consider the isotropic/zonal test signal $f_{z,r,\tau}: \mathbb{S}^{d-1} \rightarrow \mathbb{R}$ given by

$$f_{z,r,\tau}(\eta) = \tilde{f}_{\cos r,\tau}(\langle \eta, z \rangle), \quad \tilde{f}_{t_0,\tau}(t) := \begin{cases} (t - t_0)^\tau, & t \in [t_0, 1], \\ 0, & t \in [-1, t_0]. \end{cases} \quad (38)$$

In particular, $f_{z,r,\tau}$ is smooth except for a discontinuity in the r -th derivative at the boundary $\partial C(z, r)$ of the spherical cap $C(z, r)$. For $\tau = 0$, the test signal is just the characteristic function of $C(z, r)$, i.e., $f_{z,r,0} = \mathbf{1}_{C(z,r)}$. In the following, we will assume that $z = e^d$. Also, we will use the simplified notation $f_{r,\tau} := f_{e^d,r,\tau}$.

According to the discussion following Figure 1 in Section 3, the curvelet Ψ_C^j is localized at e^d and decays fastest along the directions $\pm e^{d-1}$. Consequently, for $\nu \in \mathbb{S}^{d-1}$, the rotated curvelet $T^d(g_\nu^{-1})\Psi_C^j$ is localized at $g_\nu^{-1}e^d$ and decays fastest along the directions $\pm g_\nu^{-1}e^{d-1}$. It is reasonable to expect that the frame coefficients $|\langle f_{r,\tau}, T^d(g_\nu^{-1})\Psi_C^j \rangle_{\mathbb{S}^{d-1}}|$ take their largest values when the curvelet $T^d(g_\nu^{-1})\Psi_C^j$ matches the boundary $\partial C(e^d, r)$ sufficiently well in terms of position and orientation. Here, we note that $T^d(g_\nu^{-1})\Psi_C^j$ is positioned exactly on a (higher-order) singularity of $f_{r,\tau}$ if and only if

$$\langle g_\nu^{-1}e^d, e^d \rangle = \nu_d = \cos r. \quad (39)$$

Moreover, provided that $\nu \neq \pm e^d$, the curvelet $T^d(g_\nu^{-1})\Psi_C^j$ aligns exactly with the orientation of the boundary $\partial C(e^d, r)$ whenever

$$g_\nu^{-1}e^{d-1} = \pm \frac{e^d - \langle e^d, g_\nu^{-1}e^d \rangle g_\nu^{-1}e^d}{\|e^d - \langle e^d, g_\nu^{-1}e^d \rangle g_\nu^{-1}e^d\|_2}. \quad (40)$$

Multiplying with g_ν from the left on both sides of (40), a simple calculation shows that (40) is equivalent to

$$\nu_{d-1}^2 + \nu_d^2 = 1, \quad \text{i.e.,} \quad \nu = (0, \dots, 0, \nu_{d-1}, \nu_d). \quad (41)$$

Thus, combining (39) and (41), the curvelet $T^d(g_\nu^{-1})\Psi_C^j$ matches some part of the boundary $\partial C(e^d, r)$ perfectly, in terms of position and orientation, if

$$\nu = (0, \dots, 0, \pm \sin r, \cos r).$$

In the following, we will show that the curvelet coefficients $\langle f_{r,\tau}, T^d(g_\nu^{-1})\Psi_C^j \rangle_{\mathbb{S}^{d-1}}$ peak when ν is sufficiently close to $(0, \dots, 0, \pm \sin r, \cos r)$. Otherwise, the inner products decay rapidly as j increases.

6.1 Some auxiliary results

Before we present the main theorems of this section, we need to establish some auxiliary results. The following lemma provides useful asymptotic formulas for the harmonic coefficients of the test signal defined in (38).

Lemma 6.1

Let $\lambda = \frac{d-2}{2}$. It holds that

$$\langle f_{r,\tau}, Y_k^{d,n} \rangle_{\mathbb{S}^{d-1}} = \delta_{k,0} b_n^\lambda(\tilde{f}_{\cos r,\tau}) \sqrt{\frac{\Gamma(n+d-2)(d-2)}{n!\Gamma(d-2)(2n+d-2)}}. \quad (42)$$

Here, the Gegenbauer coefficients $b_n^\lambda(\tilde{f}_{\cos r,\tau})$ are defined by (9). Moreover, if

$$\gamma(\lambda, r, \tau) = \frac{4^\lambda \Gamma(\lambda)^2 \Gamma(\lambda + \frac{1}{2}) \sqrt{\lambda} \tau! (\sin r)^{\lambda+\tau}}{2^{\tau+1/2} \pi^{3/2} \Gamma(2\lambda)^{3/2}},$$

then, for each $\varepsilon > 0$, the asymptotic expressions

$$\langle f_{r,\tau}, Y_0^{d,n} \rangle_{\mathbb{S}^{d-1}} = \gamma(\lambda, r, \tau) n^{-\tau-1} \cos((n+\lambda)r - (\lambda+\tau+1)\pi/2) + \mathcal{O}(n^{-\tau-2}), \quad (43)$$

$n \rightarrow \infty$, and

$$\langle f_{r,\tau}, Y_0^{d,n} \rangle_{\mathbb{S}^{d-1}} = \Re \left\{ e^{inr} \sum_{p=0}^{q-1} \phi_p(r) n^{-\tau-p-1} \right\} + \mathcal{O}(n^{-\tau-q-1}), \quad n \rightarrow \infty, \quad (44)$$

hold uniformly for all $r \in [\varepsilon, \pi - \varepsilon]$. Here, ϕ_p , $p = 0, \dots, q-1$, are continuous complex-valued functions.

Proof. Writing down the Gegenbauer expansion (8) of $\tilde{f}_{\cos r,\tau} \in L^2([-1, 1], w_\lambda)$ and utilizing the addition theorem for spherical harmonics, we find that

$$f_{z,r,\tau}(\eta) = \sum_{n=0}^{\infty} b_n^\lambda(\tilde{f}_{\cos r,\tau}) C_n^\lambda(\langle \eta, z \rangle) = \sum_{n=0}^{\infty} \sum_{k \in \mathcal{I}_n^d} b_n^\lambda(\tilde{f}_{\cos r,\tau}) \frac{\lambda}{n+\lambda} \overline{Y_k^{d,n}(z)} Y_k^{d,n}(\eta).$$

Thus, for $z = e^d$, formula (42) follows immediately from

$$Y_k^{d,n}(e^d) = \delta_{k,0} \sqrt{\frac{\Gamma(n+d-2)(2n+d-2)}{n!\Gamma(d-1)}},$$

which can be verified using (4) and (5).

As discussed in [22, Lemma 4], it holds that

$$\begin{aligned} \int_{\cos r}^1 (t - \cos r)^\tau C_n^\lambda(t) w_\lambda(t) dt &= \frac{\Gamma(n+2\lambda)\Gamma(\lambda+1/2)}{\Gamma(2\lambda)\Gamma(n+\lambda+1/2)} \\ &\times \frac{(n-\tau-1)! \tau!}{2^{\tau+1} n!} P_{n-\tau-1}^{(\lambda+\tau+1/2, \lambda+\tau+1/2)}(\cos r) (\sin r)^{2\lambda+2\tau+1}, \end{aligned} \quad (45)$$

as well as

$$P_{n-\tau-1}^{(\lambda+\tau+1/2, \lambda+\tau+1/2)}(\cos r) = \sqrt{\frac{2}{\pi(n-\tau-1)}} (\sin r)^{-\lambda-\tau-1} \cos((n+\lambda)r - (\lambda+\tau+1)\pi/2) + \mathcal{O}(n^{-3/2}), \quad n \rightarrow \infty, \quad (46)$$

and

$$P_{n-\tau-1}^{(\lambda+\tau+1/2, \lambda+\tau+1/2)}(\cos r) = \Re \left\{ e^{inr} \sum_{p=0}^{q-1} \phi_p(r) n^{-p-1/2} \right\} + \mathcal{O}(n^{-q-1/2}), \quad n \rightarrow \infty. \quad (47)$$

Here, the ϕ_p are continuous complex-valued functions and both asymptotic expressions hold uniformly for all $r \in [\delta, \pi - \delta]$, whenever $\delta > 0$. Combining (42) and (45), we obtain

$$\langle f_{r,\tau}, Y_k^{d,n} \rangle_{\mathbb{S}^{d-1}} = \delta_{k,0} \frac{4^\lambda \sqrt{\lambda} \Gamma^2(\lambda) \Gamma(\lambda + \frac{1}{2}) \tau! (\sin r)^{2\lambda+2\tau+1}}{2^{\tau+1} \pi \Gamma(2\lambda)^{3/2}} \times \frac{\sqrt{\Gamma(n+2\lambda)(n+\lambda)(n-\tau-1)!}}{\sqrt{n!} \Gamma(n+\lambda+\frac{1}{2})} P_{n-\tau-1}^{(\lambda+\tau+1/2, \lambda+\tau+1/2)}(\cos r). \quad (48)$$

Finally, inserting (46) and (47) into (48), it is straightforward to verify the asymptotic formulas (43) and (44). \square

Another helpful harmonic representation is given by the following lemma.

Lemma 6.2

For $\nu \in \mathbb{S}^{d-1}$, it holds that

$$\langle T^d(g_\nu^{-1}) \Psi_C^j, Y_0^{d,n} \rangle_{\mathbb{S}^{d-1}} = \sqrt{2} \kappa \left(\frac{n}{2^{j-1}} \right) A_{(n,\dots,n)}^n |\nu_d + i\nu_{d-1}|^n \cos(n \operatorname{Arg}(\nu_d + i\nu_{d-1})), \quad (49)$$

where

$$A_{(n,\dots,n)}^n = \frac{n^{(d-2)/4}}{\sqrt{\Gamma(\frac{d}{2})}} \left(\sum_{p=0}^{q-1} c_p n^{-p} + \mathcal{O}(n^{-q}) \right), \quad n \rightarrow \infty, \quad (50)$$

with $c_0 = 1$.

Proof. By (14), we have

$$\Psi_C^j(x) = \sqrt{2} \sum_{n=0}^{\infty} \sqrt{\dim \mathcal{H}_n^d} \kappa \left(\frac{n}{2^{j-1}} \right) A_{(n,\dots,n)}^n H_n(x),$$

where $H_n(x) = \Re\{(x_d + ix_{d-1})^n\}$, for $x \in \mathbb{S}^{d-1}$. Since, by construction, H_n is a multiple of $Y_{(n,\dots,n)}^{d,n} + Y_{(n,\dots,n)-}^{d,n}$, it is clear that $H_n \in \mathcal{H}_n^d$. Thus, $T^d(g_\nu^{-1})H_n \in \mathcal{H}_n^d$, for each $\nu \in \mathbb{S}^{d-1}$.

In order to verify (49), it suffices to show that

$$\sqrt{\dim \mathcal{H}_n^d} \langle T^d(g_\nu^{-1})H_n, Y_0^{d,n} \rangle_{\mathbb{S}^{d-1}} = \Re\{(\nu_d + i\nu_{d-1})^n\}.$$

Here, we first note that

$$\sqrt{\dim \mathcal{H}_n^d} Y_0^{d,n}(x) = \frac{2n+d-2}{d-2} C_n^{\frac{d-2}{2}}(\langle x, e^d \rangle).$$

Also, the map

$$(x, y) \mapsto \frac{2n + d - 2}{d - 2} C_n^{\frac{d-2}{2}}(\langle x, y \rangle)$$

represents the reproducing kernel of \mathcal{H}_n^d , which is a direct consequence of the addition theorem (7). It follows that

$$\sqrt{\dim \mathcal{H}_n^d} \langle T^d(g_\nu^{-1})H_n, Y_0^{d,n} \rangle_{\mathbb{S}^{d-1}} = T^d(g_\nu^{-1})H_n(e^d) = H_n(\nu).$$

This completes the proof of (49).

Finally, the asymptotic expression (50) can easily be derived from (22). \square

6.2 Main results

For our first main result, we assume that the rotated curvelet $T^d(g_\nu^{-1})\Psi_C^j$ matches the orientation of the boundary $\partial C(e^d, r)$ perfectly. According to the discussion in the beginning of this section, this means that $\nu_{d-1}^2 + \nu_d^2 = 1$. In this case, the following theorem provides valuable insight into the behavior of the frame coefficients $\langle f_{r,\tau}, T^d(g_\nu^{-1})\Psi_C^j \rangle_{\mathbb{S}^{d-1}}$ when $T^d(g_\nu^{-1})\Psi_C^j$ moves towards, and away from, a (higher-order) singularity of $f_{r,\tau}$. In particular, we obtain a lower bound which states that the coefficients exceed a certain threshold whenever the curvelet is positioned close enough (depending on the scale j) to the boundary $\partial C(e^d, r)$.

We note that, in the case where $\nu_{d-1}^2 + \nu_d^2 = 1$, the geodesic distance between the North Pole and the center of $T^d(g_\nu^{-1})\Psi_C^j$ takes the form

$$\text{dist}(e^d, g_\nu^{-1}e^d) = \arccos \nu_d = |\text{Arg}(\nu_d + i\nu_{d-1})|.$$

Hence, the quantity $|\text{Arg}(\nu_d + i\nu_{d-1})| - r$ indicates how far the curvelet $T^d(g_\nu^{-1})\Psi_C^j$ is from the nearest (higher-order) singularity.

The following theorem is inspired by a one-dimensional result from [22, Theorem 2], and it was previously obtained in [29, Theorem 3.3] for the two-dimensional case.

Theorem 6.3

Let $\varepsilon > 0$, $\lambda = \frac{d-2}{2}$, $\varphi = (\lambda + \tau + 1)\pi/2 - \lambda r$, and let

$$\rho(\lambda, r, \tau) = \frac{(2\pi)^{\tau-(d-2)/4} \gamma(\lambda, r, \tau)}{\sqrt{2\Gamma(\frac{d}{2})}},$$

where $\gamma(\lambda, r, \tau)$ is as defined in Lemma 6.1. Additionally, let $\nu \in \mathbb{S}^{d-1}$ with $\nu_d^2 + \nu_{d-1}^2 = 1$ and let $r \in [\varepsilon, \pi - \varepsilon]$. There exists a constant $c_0 > 0$ such that

$$\begin{aligned} & 2^{j(\tau-(d-2)/4)} \langle f_{r,\tau}, T^d(g_\nu^{-1})\Psi_C^j \rangle_{\mathbb{S}^{d-1}} \\ &= \rho(\lambda, r, \tau) \int_0^{2\pi} \kappa(t/\pi) t^{(d-2)/4-\tau-1} \cos\left(\frac{2^j t (|\text{Arg}(\nu_d + i\nu_{d-1})| - r)}{2\pi} + \varphi\right) dt + E^j(\nu), \end{aligned} \tag{51}$$

where

$$|E^j(\nu)| \leq c_0 2^{-j}.$$

Moreover, there exist constants $c_1, j_0 > 0$ as well as some nonempty open interval $I \subset [0, \infty)$ such that

$$2^{j(\tau-(d-2)/4)} |\langle f_{r,\tau}, T^d(g_\nu^{-1})\Psi_C^j \rangle_{\mathbb{S}^{d-1}}| \geq c_1, \quad \text{if } 2^j ||\text{Arg}(\nu_d + i\nu_{d-1})| - r| \in I, \quad j \geq j_0. \quad (52)$$

The dependencies of the constants are $c_0 = c_0(\kappa, \varepsilon, \tau)$, $c_1 = c_1(\kappa, \varepsilon, \tau)$, $j_0 = j_0(\kappa, \varepsilon, \tau)$, and $I = I(\kappa, \tau)$. In particular, none of the constants depend on ν .

Proof. The following proof uses methods very similar to those in the one-dimensional setting [22]. For $\nu_d^2 + \nu_{d-1}^2 = 1$, Lemma 6.1 and Lemma 6.2 yield

$$\begin{aligned} & \langle f_{r,\tau}, T^d(g_\nu^{-1})\Psi_C^j \rangle_{\mathbb{S}^{d-1}} \\ &= \frac{\gamma(\lambda, r, \tau)}{\sqrt{2^{-1}\Gamma(\frac{d}{2})}} \sum_{n=0}^{\infty} \kappa\left(\frac{n}{2^{j-1}}\right) n^{(d-2)/4-\tau-1} \cos(n \text{Arg}(\nu_d + i\nu_{d-1})) \cos(nr - \varphi) \\ &+ \mathcal{O}(2^{j((d-2)/4-\tau-1)}), \quad j \rightarrow \infty. \end{aligned}$$

Also, by Lemma 6.2, the value of $\langle f_{r,\tau}, T^d(g_\nu^{-1})\Psi_C^j \rangle_{\mathbb{S}^{d-1}}$ does not depend on the sign of $\text{Arg}(\nu_d + i\nu_{d-1})$. Hence, for the remainder of the proof we can assume that $\text{Arg}(\nu_d + i\nu_{d-1}) \in [0, \pi]$. A straightforward calculation shows that

$$\begin{aligned} & \frac{\gamma(\lambda, r, \tau)}{\sqrt{2^{-1}\Gamma(\frac{d}{2})}} \sum_{n=0}^{\infty} \kappa\left(\frac{n}{2^{j-1}}\right) n^{(d-2)/4-\tau-1} \cos(n \text{Arg}(\nu_d + i\nu_{d-1})) \cos(nr - \varphi) \\ &= 2^{j((d-2)/4-\tau)} \frac{2\pi\rho(\lambda, r, \tau)}{2^j} \sum_{n=0}^{2^j} \kappa_\tau\left(\frac{2\pi n}{2^j}\right) \cos(n(\text{Arg}(\nu_d + i\nu_{d-1}) - r) + \varphi) \\ &+ 2^{j((d-2)/4-\tau)} \frac{2\pi\rho(\lambda, r, \tau)}{2^j} \sum_{n=0}^{2^j} \kappa_\tau\left(\frac{2\pi n}{2^j}\right) \cos(n(\text{Arg}(\nu_d + i\nu_{d-1}) + r) - \varphi), \end{aligned}$$

where

$$\kappa_\tau(t) = \kappa(t/\pi)t^{\frac{d-2}{4}-\tau-1}.$$

Applying [22, Lemma 5], we obtain

$$\begin{aligned} & \frac{1}{2^j} \sum_{n=0}^{2^j} \kappa_\tau\left(\frac{2\pi n}{2^j}\right) \cos(n(\text{Arg}(\nu_d + i\nu_{d-1}) - r) + \varphi) \\ &= \frac{1}{2\pi} \int_0^{2\pi} \kappa_\tau(t) \cos\left(\frac{2^j t(\text{Arg}(\nu_d + i\nu_{d-1}) - r)}{2\pi} + \varphi\right) dt + \mathcal{O}(2^{-jq}). \end{aligned}$$

Similarly, [22, Lemma 5] combined with repeated integration by parts shows that

$$\frac{1}{2^j} \sum_{n=0}^{2^j} \kappa_\tau\left(\frac{2\pi n}{2^j}\right) \cos(n(\text{Arg}(\nu_d + i\nu_{d-1}) + r) - \varphi) = \mathcal{O}(2^{-jq}).$$

This completes the proof of (51).

To verify (52), we note that the map

$$z \mapsto \int_0^{2\pi} \kappa(t/\pi)t^{(d-2)/4-\tau-1} \cos(zt + \varphi) dt$$

is an entire function. Thus, a corresponding interval which is free of zeroes must exist. \square

Theorem 6.3 implies, in particular, that the curvelet coefficients exceed a certain threshold whenever the analysis function sufficiently matches the boundary $\partial C(e^d, r)$. We now establish a second result, showing that the values $|\langle f_{r,\tau}, T^d(g_\nu^{-1})\Psi_C^j \rangle_{\mathbb{S}^{d-1}}|$ decay rapidly when the curvelet is either away from a singularity or not aligned with the orientation of $\partial C(e^d, r)$. Otherwise, if $T^d(g_\nu^{-1})\Psi_C^j$ matches the boundary in terms of position and orientation, the upper bound given by the following theorem is consistent with the lower bound from **Theorem 6.3**. Again, the following estimate is motivated by a previous one-dimensional result from [22, Theorem 2], and a two-dimensional version was previously established in [29, Theorem 3.3].

Theorem 6.4

Let $\varepsilon > 0$ and let Ψ_C^j , $j \in \mathbb{N}_0$, be as defined in **Section 3** with $\kappa \in C^q([0, \infty))$, for some $q \in \mathbb{N}$. We assume that there is some $t_0 \in (1/2, 2)$ such that $\kappa^{(q)}(t) \neq 0$ for each $t \in (1/2, t_0)$. Then there exists a constant $c_2 = c_2(\kappa, \varepsilon, \tau, q) > 0$ such that

$$2^{j(\tau-(d-2)/4)} |\langle f_{r,\tau}, T^d(g_\nu^{-1})\Psi_C^j \rangle_{\mathbb{S}^{d-1}}| \leq \frac{c_2 |\nu_d + i\nu_{d-1}|^{2j-2}}{(1 + 2^j |r - |\text{Arg}(\nu_d + i\nu_{d-1})||)^q},$$

for all $\nu \in \mathbb{S}^{d-1}$, provided that $r \in [\varepsilon, \pi - \varepsilon]$.

Proof. Applying **Lemma 6.1** and **Lemma 6.2**, we obtain

$$\begin{aligned} & 2^{j(\tau-(d-2)/4)} \langle f_{r,\tau}, T^d(g_\nu^{-1})\Psi_C^j \rangle_{\mathbb{S}^{d-1}} \\ &= \Re \left\{ \sum_{p=0}^{q-1} \frac{\phi_p(r)}{2^{j(1+p)}} \sum_{n=0}^{\infty} \kappa_{\tau,p} \left(\frac{n}{2^{j-1}} \right) \exp(inr) \cos(n \text{Arg}(\nu_d + i\nu_{d-1})) \right\} + E^j(\nu), \end{aligned}$$

where $\kappa_{\tau,p}(t) = \kappa(t)t^{(d-2)/4-p-\tau-1}z^{2^{j-1}t}$, $z = |\nu_d + i\nu_{d-1}|$, and

$$|E^j(\nu)| \leq c |\nu_d + i\nu_{d-1}|^{2j-2} 2^{-jq}.$$

The assertion now follows from the same arguments that we used to verify (23) in the proof of **Theorem 4.1**. \square

Combining **Theorem 6.3** and **Theorem 6.4**, it follows that the (higher-order) singularities of $f_{r,\tau}$ can be identified precisely, in terms of position and orientation, by the asymptotic decay of the frame coefficients $\langle f_{r,\tau}, T^d(g)\Psi_C^j \rangle_{\mathbb{S}^{d-1}}$. In particular,

$$\sup_{g \in SO(d)} |\langle f_{r,\tau}, T^d(g)\Psi_C^j \rangle_{\mathbb{S}^{d-1}}| \sim 2^{-j(\tau-(d-2)/4)}.$$

Appendix

In the following, we briefly review some fundamentals of harmonic analysis on $SO(d)$. All formulas presented here can be found in classical literature such as [32]. We also refer to our recent discussions in [14, 30].

Let μ_d denote the Haar measure on $SO(d)$ with the normalization

$$\int_{SO(d)} d\mu_d = 1.$$

Each element $g \in SO(d)$ can be written as $g = g_\eta h$, where $h \in SO(d-1)$ and $g_\eta \in SO(d)$ with $g_\eta e^d = \eta \in \mathbb{S}^{d-1}$. Clearly, this representation is not unique. However, independent of the choice of g_η and h , it holds that

$$\int_{SO(d)} f(g) d\mu_d(g) = \int_{\mathbb{S}^{d-1}} \int_{SO(d-1)} f(g_\eta h) d\mu_{d-1}(h) d\omega_{d-1}(\eta), \quad (\text{A.1})$$

for each $f \in L^1(SO(d))$. Here, due to the invariance of the Haar measure μ_{d-1} on $SO(d-1)$, the inner integral on the right-hand side does not depend on the choice of g_η .

We now consider the unitary group representation

$$g \mapsto T^d(g), \quad T^d(g)f(x) = f(g^{-1}x),$$

of $SO(d)$ on $L^2(\mathbb{S}^{d-1})$. Its subrepresentations on the spaces \mathcal{H}_n^d are irreducible. Consequently, as part of the famous Peter-Weyl theorem, the matrix functions $t_{k,m}^{d,n} : SO(d) \rightarrow \mathbb{C}$ given by

$$t_{k,m}^{d,n}(g) = \langle T^d(g)Y_m^{d,n}, Y_k^{d,n} \rangle_{\mathbb{S}^{d-1}}, \quad k, m \in \mathcal{I}_n^d, \quad n \in \mathbb{N}_0, \quad (\text{A.2})$$

form an orthogonal system for $L^2(SO(d))$ w.r.t. the inner product

$$\langle f_1, f_2 \rangle_{SO(d)} = \int_{SO(d)} f_1 \overline{f_2} d\mu_d.$$

Moreover,

$$\int_{SO(d)} |t_{k,m}^{d,n}|^2 d\mu_d = \frac{1}{\dim \mathcal{H}_n^d}.$$

It is not difficult to verify that the matrix functions in (A.2) satisfy the symmetry

$$\overline{t_{k,\ell}^{d,n}(g)} = t_{k^-, \ell^-}^{d,n}(g), \quad (\text{A.3})$$

where $(k_1, \dots, k_{d-3}, k_{d-2})^-$ is defined as $(k_1, \dots, k_{d-3}, -k_{d-2})$. Similarly, it is easy to see that

$$t_{k,\ell}^{d,n}(g^{-1}) = t_{\ell^-, k^-}^{d,n}(g). \quad (\text{A.4})$$

It is obvious that (A.2) can also be written as

$$Y_m^{d,n}(g^{-1}\eta) = \sum_{k \in \mathcal{I}_n^d} t_{k,m}^{d,n}(g) Y_k^{d,n}(\eta), \quad \eta \in \mathbb{S}^{d-1}. \quad (\text{A.5})$$

The fact that T^d is a group homomorphism, i.e., $T^d(g\tilde{g}) = T^d(g)T^d(\tilde{g})$, where each $T^d(g)$ is a unitary operator on $L^2(\mathbb{S}^{d-1})$, implies the addition formula

$$t_{k,\ell}^{d,n}(g\tilde{g}) = \sum_{m \in \mathcal{I}_n^d} t_{k,m}^{d,n}(g) t_{m,\ell}^{d,n}(\tilde{g}), \quad g, \tilde{g} \in SO(d). \quad (\text{A.6})$$

Choosing $\eta = e^d$ in (A.5), a simple calculation yields

$$\overline{Y_m^{d,n}(e^d)} = \sum_{k \in \mathcal{I}_n^d} \overline{Y_k^{d,n}(e^d)} t_{m,k}^{d,n}(g_\nu). \quad (\text{A.7})$$

In particular, spherical harmonics are linear combinations of certain matrix functions, as $\overline{t_{m,k}^{d,n}}$ is clearly a linear combination of the $t_{r,s}^{d,n}$, $r, s \in \mathcal{I}_n^d$.

Matrix functions of different dimensions are intimately connected. Specifically, we have

$$t_{k,\ell}^{d,n}(h) = \delta_{k_1,\ell_1} t_{(k_2,\dots,k_{d-2}),(\ell_2,\dots,\ell_{d-2})}^{d-1,k_1}(h), \quad h \in SO(d-1), \quad d \geq 4, \quad (\text{A.8})$$

as well as

$$t_{k,\ell}^{3,n}(h(\gamma)) = \delta_{k,\ell} \exp(ik\gamma), \quad \gamma \in [0, 2\pi), \quad (\text{A.9})$$

where $h(\gamma) \in \mathbb{R}^{3 \times 3}$ is a positive rotation by γ in the (x_1, x_2) -plane.

For $N \in \mathbb{N}_0$, let

$$\mathcal{M}_N^1(SO(d)) = \text{span}\{t_{k,m}^{d,n}, k, m \in \mathcal{I}_n^d, 0 \leq n \leq N\}. \quad (\text{A.10})$$

Here, the upper index 1 in the notation $\mathcal{M}_N^1(SO(d))$ refers to the fact that this space is spanned by class 1 matrix functions (see [32] for more details).

Literature

- [1] Askari-Hemmat, A., Dehghan, M. A., and Skopina, M. “Polynomial Wavelet-Type Expansions on the Sphere”. In: *Math. Notes* 74.1 (2003), pp. 278–285. DOI: [10.1023/A:1025016510773](https://doi.org/10.1023/A:1025016510773).
- [2] Aslam, A., Khalid, Z., and McEwen, J. D. “Multiscale Optimal Filtering on the Sphere”. In: *IEEE Signal Process. Lett.* 28 (2021), pp. 394–398. DOI: [10.1109/lsp.2021.3056236](https://doi.org/10.1109/lsp.2021.3056236).
- [3] Atkinson, K. and Han, W. *Spherical harmonics and approximations on the unit sphere. An introduction*. Vol. 2044. Lect. Notes Math. Berlin: Springer, 2012. DOI: [10.1007/978-3-642-25983-8](https://doi.org/10.1007/978-3-642-25983-8).
- [4] Bannai, E. and Bannai, E. “A survey on spherical designs and algebraic combinatorics on spheres”. In: *Eur. J. Comb.* 30.6 (2009), pp. 1392–1425. DOI: [10.1016/j.ejc.2008.11.007](https://doi.org/10.1016/j.ejc.2008.11.007).
- [5] Bartel, F., Kämmerer, L., Pozharska, K., Schäfer, M., and Ullrich, T. “Exact discretization, tight frames and recovery via D -optimal designs”. In: *SMAI J. Comput. Math.* 11 (2025), pp. 607–636. DOI: [10.5802/smai-jcm.136](https://doi.org/10.5802/smai-jcm.136).
- [6] Bondarenko, A., Radchenko, D., and Viazovska, M. “Optimal asymptotic bounds for spherical designs”. In: *Ann. Math. (2)* 178.2 (2013), pp. 443–452. DOI: [10.4007/annals.2013.178.2.2](https://doi.org/10.4007/annals.2013.178.2.2).
- [7] Brown, G. and Dai, F. “Approximation of smooth functions on compact two-point homogeneous spaces”. In: *J. Funct. Anal.* 220.2 (2005), pp. 401–423. DOI: [10.1016/j.jfa.2004.10.005](https://doi.org/10.1016/j.jfa.2004.10.005).
- [8] Cai, X., Wallis, C. G. R., Chan, J. Y. H., and McEwen, J. D. “Wavelet-based segmentation on the sphere”. In: *Pattern Recognit.* 100 (2020), p. 107081. DOI: [10.1016/j.patcog.2019.107081](https://doi.org/10.1016/j.patcog.2019.107081).
- [9] Chan, J. Y. H., Leistedt, B., Kitching, T. D., and McEwen, J. D. “Second-Generation Curvelets on the Sphere”. In: *IEEE Trans. Signal Process.* 65.1 (2017), pp. 5–14. DOI: [10.1109/TSP.2016.2600506](https://doi.org/10.1109/TSP.2016.2600506).
- [10] Dai, F. “Characterizations of function spaces on the sphere using frames”. In: *Trans. Am. Math. Soc.* 359.2 (2007), pp. 567–589. DOI: [10.1090/S0002-9947-06-04030-X](https://doi.org/10.1090/S0002-9947-06-04030-X).

- [11] Dai, F. and Xu, Y. *Approximation theory and harmonic analysis on spheres and balls*. Springer Monogr. Math. New York, NY: Springer, 2013. DOI: [10.1007/978-1-4614-6660-4](https://doi.org/10.1007/978-1-4614-6660-4).
- [12] Delsarte, P., Goethals, J. M., and Seidel, J. J. “Spherical codes and designs”. In: *Geom. Dedicata* 6 (1977), pp. 363–388. DOI: [10.1007/BF03187604](https://doi.org/10.1007/BF03187604).
- [13] Durastanti, C., Marinucci, D., and Todino, A. P. “Flexible-bandwidth needlets”. In: *Bernoulli* 30.1 (2024), pp. 22–45. DOI: [10.3150/22-BEJ1513](https://doi.org/10.3150/22-BEJ1513).
- [14] Hasannasab, M., Kaldewey, L., and Schoppert, F. “Directional polynomial frames on spheres”. Preprint. 2026. arXiv: [2601.15883](https://arxiv.org/abs/2601.15883) [[math.CA](https://arxiv.org/abs/2601.15883)].
- [15] McEwen, J. D., Feeney, S. M., Peiris, H. V., Wiaux, Y., Ringeval, C., and Bouchet, F. R. “Wavelet-Bayesian inference of cosmic strings embedded in the cosmic microwave background”. In: *Mon. Not. R. Astron. Soc.* 472.4 (2017), pp. 4081–4098. DOI: [10.1093/mnras/stx2268](https://doi.org/10.1093/mnras/stx2268).
- [16] McEwen, J. D., Durastanti, C., and Wiaux, Y. “Localisation of directional scale-discretised wavelets on the sphere”. In: *Appl. Comput. Harmon. Anal.* 44.1 (2018), pp. 59–88. DOI: [10.1016/j.acha.2016.03.009](https://doi.org/10.1016/j.acha.2016.03.009).
- [17] McEwen, J. D., Vandergheynst, P., and Wiaux, Y. “On the computation of directional scale-discretized wavelet transforms on the sphere”. In: *Wavelets and Sparsity XV*. Vol. 8858. SPIE, 2013, p. 88580I. DOI: [10.1117/12.2022889](https://doi.org/10.1117/12.2022889).
- [18] Mhaskar, H. N. “Polynomial operators and local smoothness classes on the unit interval”. In: *J. Approx. Theory* 131.2 (2004), pp. 243–267. DOI: [10.1016/j.jat.2004.10.002](https://doi.org/10.1016/j.jat.2004.10.002).
- [19] Mhaskar, H. N. “On the representation of smooth functions on the sphere using finitely many bits”. In: *Appl. Comput. Harmon. Anal.* 18.3 (2005), pp. 215–233. DOI: [10.1016/j.acha.2004.11.004](https://doi.org/10.1016/j.acha.2004.11.004).
- [20] Mhaskar, H. N., Narcowich, F. J., Prestin, J., and Ward, J. D. “Polynomial frames on the sphere”. In: *Adv. Comput. Math.* 13.4 (2000), pp. 387–403. DOI: [10.1023/A:1016639802349](https://doi.org/10.1023/A:1016639802349).
- [21] Mhaskar, H. N., Narcowich, F. J., and Ward, J. D. “Spherical Marcinkiewicz-Zygmund inequalities and positive quadrature”. In: *Math. Comput.* 70.235 (2001), pp. 1113–1130. DOI: [10.1090/S0025-5718-00-01240-0](https://doi.org/10.1090/S0025-5718-00-01240-0).
- [22] Mhaskar, H. N. and Prestin, J. “Polynomial frames for the detection of singularities”. In: *Wavelet analysis and multiresolution methods. Proceedings of the conference, University of Illinois, Urbana-Champaign, IL, USA*. New York, NY: Marcel Dekker, 2000, pp. 273–298. DOI: [10.1201/9781482290066-19](https://doi.org/10.1201/9781482290066-19).
- [23] Müller, C. *Spherical harmonics*. Vol. 17. Lect. Notes Math. Springer, Cham, 1966. DOI: [10.1007/BFb0094775](https://doi.org/10.1007/BFb0094775).
- [24] Narcowich, F. J., Petrushev, P., and Ward, J. D. “Decomposition of Besov and Triebel-Lizorkin spaces on the sphere”. In: *J. Funct. Anal.* 238.2 (2006), pp. 530–564. DOI: [10.1016/j.jfa.2006.02.011](https://doi.org/10.1016/j.jfa.2006.02.011).
- [25] Narcowich, F. J., Petrushev, P., and Ward, J. D. “Localized Tight Frames on Spheres”. In: *SIAM J. Math. Anal.* 38.2 (2006), pp. 574–594. DOI: [10.1137/040614359](https://doi.org/10.1137/040614359).

- [26] Petrushev, P. and Xu, Y. “Localized polynomial frames on the interval with Jacobi weights”. In: *J. Fourier Anal. Appl.* 11.5 (2005), pp. 557–575. DOI: [10.1007/s00041-005-4072-3](https://doi.org/10.1007/s00041-005-4072-3).
- [27] Price, M. A., McEwen, J. D., Pratley, L., and Kitching, T. D. “Sparse Bayesian mass-mapping with uncertainties: Full sky observations on the celestial sphere”. In: *Mon. Not. R. Astron. Soc.* 500.4 (2020), pp. 5436–5452. DOI: [10.1093/mnras/staa3563](https://doi.org/10.1093/mnras/staa3563).
- [28] Rogers, K. K., Peiris, H. V., Leistedt, B., McEwen, J. D., and Pontzen, A. “SILC: a new Planck internal linear combination CMB temperature map using directional wavelets”. In: *Mon. Not. R. Astron. Soc.* 460.3 (2016), pp. 3014–3028. DOI: [10.1093/mnras/stw1121](https://doi.org/10.1093/mnras/stw1121).
- [29] Schoppert, F. “Direction sensitive analysis of higher order jump discontinuities along circles on the sphere”. In: *GEM. Int. J. Geomath.* 14 (2023), p. 33. DOI: [10.1007/s13137-023-00217-w](https://doi.org/10.1007/s13137-023-00217-w).
- [30] Schoppert, F. “Directional Polynomial Wavelets on Spheres”. In: *J. Fourier Anal. Appl.* 32.1 (2025), p. 3. DOI: [10.1007/s00041-025-10210-6](https://doi.org/10.1007/s00041-025-10210-6).
- [31] Schoppert, F. “Edge detection with polynomial frames on the sphere”. In: *J. Approx. Theory* 315 (2026), p. 106279. DOI: [10.1016/j.jat.2025.106279](https://doi.org/10.1016/j.jat.2025.106279).
- [32] Vilenkin, N. Y. *Special functions and the theory of group representations. Translation from the Russian by V. N. Singh*. Vol. 22. Transl. Math. Monogr. American Mathematical Society (AMS), Providence, RI, 1968. DOI: [10.1090/mmono/022](https://doi.org/10.1090/mmono/022).
- [33] Wallis, C. G. R., Wiaux, Y., and McEwen, J. D. “Sparse Image Reconstruction on the Sphere: Analysis and Synthesis”. In: *IEEE Trans. Image Process.* 26.11 (2017), pp. 5176–5187. DOI: [10.1109/tip.2017.2716824](https://doi.org/10.1109/tip.2017.2716824).
- [34] Wiaux, Y., Jacques, L., and Vandergheynst, P. “Correspondence Principle between Spherical and Euclidean Wavelets”. In: *Astrophys. J.* 632.1 (Oct. 2005), p. 15. DOI: [10.1086/432926](https://doi.org/10.1086/432926).
- [35] Wiaux, Y., McEwen, J. D., Vandergheynst, P., and Blanc, O. “Exact reconstruction with directional wavelets on the sphere”. In: *Mon. Not. Roy. Astron. Soc.* 388.2 (2008), pp. 770–788. DOI: [10.1111/j.1365-2966.2008.13448.x](https://doi.org/10.1111/j.1365-2966.2008.13448.x).
- [36] Zimbres, M., Batista, R. A., and Kemp, E. “Using spherical wavelets to search for magnetically-induced alignment in the arrival directions of ultra-high energy cosmic rays”. In: *Astropart. Phys.* 54 (2014), pp. 54–60. DOI: [10.1016/j.astropartphys.2013.11.001](https://doi.org/10.1016/j.astropartphys.2013.11.001).